/A STUDY OF THE MAGNETIC PROPERTIES OF AND INTERVALENCE ELECTRON TRANSFER IN $[Co(phen)_2]_3[Fe(CN)_6]_2*23H_2O$/

by

R. David Jones
B. A., Monmouth College, 1982

A MASTER'S THESIS

submitted in partial fulfillment of the
requirements for the degree

MASTER OF SCIENCE

Department of Chemistry

KANSAS STATE UNIVERSITY

Manhattan, Kansas

1985

Approved by:

Keith F. Purcell
Major Professor

I would like to dedicate this work to my parents, Robert C. and Judith A. Jones for supporting me through my undergraduate career. I would also like to dedicate this work to Nancy Nolan whose love and understanding made the work bearable.

Acknowledgements

I would like to thank Drs. Basil Curnutte and John Eck for their assistance with the Mossbauer spectrometer. I also acknowledge the assistance fo Donald Pivonka in obtaining the far-infrared spectrum. I would like to thank Kansas State University and the Petroleum Research Fund for their financial support. Finally, I would like to thank Dr. Keith F. Purcell for his support and guidance during this project.

Table of Contents

List of Tables

INTRODUCTION

Bright and interesting colors have been an attractive and useful feature of inorganic chemistry since it's earliest days. The discovery of the intensely colored prussian blue ($Fe_4[Fe(CN)_6]_3$) by Diesbach in 1704 is generally considered to be the inception of inorganic chemistry[1]. Prussian blue is a member of a class of compounds called mixed valence compounds. Mixed valence compounds are compounds which have two sites (atoms) which are both capable of multiple valences and for which one could construct reasonable localized electronic structures which differ by the assignment of one or two electrons at the multivalent sites. These compounds show an intervalence transition spectral band (IT band) either when one of these localized structures is higher in energy than the other (electronic transition), or, if the sites are equivalent, from high vibrational excitation. IT bands are found in the ultraviolet, visible and near infrared regions of the electromagnetic spectrum. IT bands in the visible region often result in deeply colored compounds, such as prussian blue.

Our interest in these comopunds results from the search for compounds suitable for study with time resolved emission Mossbauer spectroscopy (TREMS)[2,3]. The goal is to develop compounds that, upon electron capture conversion of a ^{57}Co nucleus to an iron nucleus, will experience electron transfer either on to or off of the newly formed iron and in the nsec to microsec time frame observable using this technique. It was conjectured by us that by forming a salt with $[Co(phen)_3]^{+3}$ and $[Fe(CN)_6]^{-4}$ that an electron would cross to the new iron center upon conversion of the cobalt to iron.

The compound resulting from the reaction of $[Co(phen)_3]^{3+}$ and $[Fe(CN)_6]^{-4}$ by previous work of this group was unexpectedly dark green in color. Furthermore, on drying of the green product over phosphorous pentoxide at 100C in vacuo the color changed to a reddish brown. Initially, the color change was not reproducible from batch to batch; the brown form would often not appear on drying. The purpose of this thesis is to 1) discover the synthetic procedures which result in a pure product with consistent behaviour, 2) determine its composition, and 3) determine the origin of the green color in the hydrated complex and explain the absence of the green color in the anhydrous form of the product. It is hoped that with this information, studies with TREMS using the compound can be undertaken.

The early chemistry of mixed valence compounds involved their use as pigments and dyes; however, in the nineteenth century, a theoretical basis for the understanding of these compounds was not available, making their synthesis more of an art than a science. In 1896, Werner[4] recognized that the transfer of an electron between metal centers of different valence caused coloration in a compound. In 1922, Wells surmised that the color was caused by the interaction of light with an electron that was oscillating between the metal atoms[5]. Stieglitz amended Well's view by noting that it was not necessary to invoke valence oscillation (resonance) to explain the origin of the absorption, but that photochemical oxidation-reduction offered a reasonable explanation[6]. The present view of mixed valence phenomena is somewhere between these two extremes.

Intervalence transition bands in mixed valence compounds are widely occurring phenomena. Compounds which exhibit them are found in biology and mineralogy. Mixed valence chemistry is pertinent to the study of photochemistry, semiconductors, and electrochemistry, among others[7].

Because transition metals exhibit multiple valences, they are fertile ground for the investigation of mixed valence chemistry.

Robin and Day[8] classified mixed valence compounds into three types, called Types I, II, and III. Type I compounds have the different valences well trapped in different sites. For example, metal A has a valence of +3 and is in an octahedral site in the lattice; metal B has a valence of +2 and is in a site of tetrahedral symmetry. This results in a poor energy match between orbitals and consequently negligible mixing of the valence orbitals on each site (delocalization of a valence electron). Type I compounds are insulators and have a vanishingly small intensity for the intervalence transition band; their electronic spectra appear to be a simple sum of the spectra for the constituent ions. An example of a type I compound is Cr_2F_5.

Type II compounds have the different valences in similar but not equivalent sites. Small, but detectable mixing of the orbitals for the two different sites is seen. Type II compounds are often characterized by an intervalence transition band which is not seen in the spectra of the constituent ions. Bands which are present in the parent species will still be apparent in the mixed valence compound, however they will often be shifted slightly from their position in the constituent ions. Type II compounds are often semiconductors. Prussian blue is a type II compound.

Type III compounds have all ions indistinguishable from each other. There is a strong mixing of the valence orbitals between centers. Constituent ion bands are not discernable in the electronic spectra. The electron is delocalized throughout the system. Type III compounds are divisible into two subclasses. Type IIIA compounds have molecular clusters in which the ions in the cluster are all equivalent. These compounds are generally insulators, electron transfer between clusters being difficult.

Type IIIB compounds have chemical equivalence for all the ions in the lattice. They are metals in that they display the characteristics of metals. Triiodide ion is type IIIA. The compounds $(La_{1-x}Ca_x)MnO_3$ are type IIIB.

The most studied mixed valence compounds contain the same element in two different valences; however, several heteroatomic mixed valence compounds are known to exist[9]. In these cases, the highest occupied orbital (HOMO) on the reducing atom and the lowest unoccupied orbital (LUMO) on the oxidizing atom must have similar energies if a visible or near-infrared intervalence transition is to be possible. As examples, Robin[10] has prepared the osmocyanide and ruthenocyanide analogs of prussian blue ($Fe_4[M(CN)_6]_3$ M = Os, Ru). Both exhibit an IT band similar to that of prussian blue.

Photo-induced outer sphere electron transfer in solution is not often seen, as the ion-pairing is usually too low to permit an observable intensity. Curtis and Meyer[11,12] have used systems in which the ions are highly charged and opposite in sign to increase the ion pair concentration. The ions used are of the form (NH_3)M1(III)L and M2(II)$(CN_6$ where M1, M2 = Fe, Ru, Os and L is pyridine, a substituted pyridine, imidazole or pyrazole. The IT band appears in the near-infrared region. A significant result was that the transfer appeared to be mediated by the NH_3 ligand orbitals, as the transition probability showed little dependence on the direct d-orbital overlap between the metals. The transfer was probably mediated through the ammines, as the other ligand had little influence on the energy or intensity of the transition. It should be noted that both heteronuclear and homonuclear types of compounds are seen in this series.

Thermal electron transfer kinetics studies have been performed in aqueous solution on the system we are using, but at low concentrations[13] (all species at 10^{-3} M to 10^{-4} M). Using the temperature jump method for the reaction:

$$[Fe(CN)_6]^{-3} + [Co(phen)_3]^{+2} \rightleftarrows [Fe(CN)_6]^{-4} + [Co(phen)_3]^{+3}$$

it was determined that K = 5 (showing Co(III)/Fe(II) is favored). k_{et} for both the forward and reverse reactions were estimated to be greater than $6 * 10^4$ sec^{-1}.

Robin and Day[8] developed a simple theoretical model on which they based their classification. Wavefunctions describing the mixed valence compound may be developed from zeroth order (localized) ground state and excited state wave functions. Given a site A occupied by a metal in the +3 oxidation state and surrounded octahedrally by six sites B which are metals in the +4 state, then the localized (zeroth order) ground state wavefunction for the cluster is:

$$1)\ \Psi_o^{(o)} = \Psi_A^{III}\ \Psi_B^{IV}\ \Psi_{B_2}^{IV}\ \Psi_{B_3}^{4} \ldots \Psi_{B_6}^{IV}$$

where Ψ_A^{III} is the wavefunction for the reduced site and $\Psi_{B_{1-6}}^{IV}$ are those of the oxidized sites. Six zeroth order excited states can then be constructed by making site A an oxidized site and each site B the reduced site and then taking linear combinations of the six possible excited wavefunctions to give:

$$2)\ \Psi_k^{(o)} = \Psi_A^{IV} \left[\sum_{j=1}^{6} C_{kj}\ \Psi_{B_1}^{IV}\ \Psi_{B_2}^{IV}\ \Psi_{Bj}^{III} \ldots \Psi_{B_6}^{IV}\right]\ k = 1,6$$

$$3)\quad \Psi_k^{(o)} = \Psi_A^{IV}\left[\sum_{j=1}^{6} C_{kj}\,\Pi_{Bj}\,\Psi_{Bj}^{III}\right]\quad k = 1,6$$

The C_{kj}'s normalize the Ψ_k's and make them transform according to the symmetry of the cluster. Π_{Bj} is the product of all the Ψ_B's in the oxidized state except Ψ_{Bj}. In the present case the $\Psi_k^{(o)}$'s break into an e_g pair, a t_{1u} triad and an a_{1g} wavefunction. If it is assumed that one of the excited state wavefuncitons, that with k = x, has the correct symmetry to mix with the zeroth ground state wave function, one can write for the first order ground state wavefunction:

$$4)\quad \Psi_o^{(1)} = 1/N[\sqrt{1-\alpha^2}\,\Psi_o^{(o)} + \alpha\,\Psi_x^{(o)}]$$

$$5)\quad \Psi_o^{(1)} = 1/N[\sqrt{1-\alpha^2}\,\Psi_A^{III}\Psi_{B_1}^{IV}\,\Psi_{B_2}^{IV}\ldots\Psi_{B_6}^{IV} + \alpha\,\Psi_A^{IV}\sum_{j=1}^{6} C_{xj}\,\Pi_{Bj}\Psi_{Bj}^{III}]$$

To simplify this, the electrons of an oxidized species can be considered to form a frozen closed shell and all but the highest energy electron in the reduced species to also form a frozen closed shell. This allows us to rewrite the Ψ_A's and Ψ_B's as:

$$6)\quad \Psi_A^{III} = \phi_A^C\phi_A \qquad 7)\quad \Psi_A^{IV} = \phi_A^C$$

$$8)\quad \Psi_B^{III} = \phi_B^C\,\phi_B \qquad 9)\quad \Psi_B^{IV} = \phi_B^C$$

Substituting back into equation 5 gives:

$$10)\quad \Psi_o^{(1)} = \frac{K}{N}\left[\sqrt{1-\alpha^2}\,\phi_A^C\,\phi_{B_1}^C\,\phi_{B_2}^C\ldots\phi_{B_6}^C\,\phi_A + \alpha\,\phi_{Aj}^C\sum_{j=1}^{b} C_{xj}\,\Pi_{Bj}\,\phi_{Bj}^C\,\phi_{Bj}\right]$$

All the closed shell wavefunctions can be factored and defined as K to give us:

$$11)\ \Psi_o^{(1)} = \frac{K}{N}\left[\sqrt{1-\alpha^2}\ \phi_A + \alpha \sum_{j=1}^{6} C_{xj}\ \phi_{Bj}\right]$$

By solving the secular equation, one can derive the value for α^2:

$$12)\ \alpha^2 = N^2\left[1-\left(1 + \frac{2E_x^2 - 2E_x\sqrt{E_x^2 + 4V^2}\ 4V^2}{4V^2}\right)^{-1}\right]$$

where E_x is the energy of $\Psi_x^{(o)}$ above the zeroth order ground state energy and V is the integral $\langle\Psi_o^{(o)}|H|\Psi_x^{(o)}\rangle$.

For very large values of E_x, α tends to zero and equation 11 reduces to the zeroth order ground state wave function. When E_x is zero the value of α^2 is $N^2/2$ and the electron is delocalized to the B sites. The first case describes the conditions under which type I behavior is seen. The orbitals are far apart in energy and the electron resides only on site A. When α is small but not zero, type II behavior arises. This can occur when E_x is small. Type III behavior occurs when E_x is zero. E_x will most likely be large when sites A and B are chemically different type sites, or when the atoms occupying the sites are not of the same element. α is also dependent upon V. Large values of V cause α^2 to approach its maximum value - $N^2/2$.

Large values of V are associated with strong mixing of $\Psi_o^{(o)}$ and $\Psi_x^{(o)}$ by direct overlap or by strong through bond coupling. This latter requires high metal-ligand covalency. Because this covalency often results in high conductivity and several low frequency absorption bands, it is difficult to identify traditional Type II phenomena in these compounds.

An equation has been developed by Hush which describes the relationship between the intensity of the absorption band and α^2.[9]

$$10) \quad \alpha^2 = 4.24 \times 10^{-4} E_{max} \Delta\bar{\nu}/d^2 \bar{\nu}_{max}$$

where E_{max} is the molar extinction coefficient at the band maximum, $\Delta\bar{\nu}$ is the full width at half height of the band, $\bar{\nu}_{max}$ is the frequency of the band maximum, and d is the distance between the sites of the transition.

Hexacyanoferrates

Iron cyanide complexes are among the oldest known metal complexes. The best known forms are the potassium salts which are readily available commercially. Potassium ferrocyanide trihydrate is a pale yellow compound with a waxy appearance. The anhydrous form is white. Potassium ferricyanide exhibits relatively large shiny red crystals. When the latter are ground up, the color changes to a bright yellow. It is also yellow in aqueous solution.

Both hexacyanoferrates are reasonably inert to aquation. Ferrocyanide undergoes aquation in the presence of light according to the following scheme:

$$[Fe(CN)_6]^{-4} + H_2O \rightleftharpoons [Fe(CN)_5H_2O]^{-3} + CN^-$$

$$CN^- + H_2O \rightleftharpoons OH^- + HCN$$

As long as the HCN remains in solution, the aquation reverses with the light is extinguished[14]. The ferricyanide ion is somewhat more labile to the loss

of cyanide than the ferrocyanide ion, even though it is more thermodynamically stable to aquation[15]. (Ferricyanide salts are toxic because of this.) Furthermore, ferricyanide undergoes reaction with the CN^- released by aquation to form ferrocyanide, cyanate and cyanogen[16].

Both hexacyanoferrates form strong acids. Ferrocyanic acid has $K_1 > K_2 > 0.1$, $K_3 = (6 \pm 2) * 10^{-3}$ and $K_4 = (6.7 \pm .3) * 10^{-5}$ [17] Ferricyanic acid is strong with respect to all three protons[18].

Ferrocyanide and ferricyanide salts are both well characterized by Mossbauer spectroscopy. Potassium ferrocyanide trihydrate shows a single line at -0.35 ± .007 mm/sec at room temperature relative to α-Fe[19]. The anhydrous form of the same salt has a single line at +.04 mm/sec. The center shift (c.s.) for potassium ferricyanide is -.12 mm/sec at room temperature[20]. The center shifts are dependent on the temperature and the cation present. As the center shifts are so similar and so cation dependent, the c.s. parameter is not useful in assigning the valence of the iron center[21]. Ferrocyanide c.s.'s range from -.171 mm/sec for the etherate of ferrocyanic acid to +.04 mm/sec for anhydrous potassium ferrocyanide at room temperature[22]. Ferricyanide center shifts range from -.18 for mm/sec cupric ferricyanide to -.097 mm/sec for stannic ferricyanide at room temperature[23]. Typically, for the same cation, the center shift for ferricyanide is less than the ferrocyanide by .1 mm/sec[24]. For monovalent cations, the center shift increases with the size of the cation[25]. Generalizations are more difficult to make in the cases of higher valent ions because of bonding of the terminal nitrogen to the cation. In a study with the trivalent cations of Al, Ga, Sc, In, and Y, a decrease in the polarizing power of M^{+3} correlated with an increase in the center shift[27]. Because the center shift is dependent on the second order doppler shift, a

more detailed treatment of the center shift requires an intimate knowledge of the lattice parameters.

Ferricyanide shows a small temperature dependent quadrupole splitting. For the potassium salt the splitting is .30 mm/sec at room temperature. This splitting decreases with increasing temperature. The splitting is caused by a Jahn-Teller distortion. The magnitude of the splitting is dependent on the cation present and the purity of the sample.

Ferricyanide electronic spectra show bands at 417, 303, and 263 nm. with shoulders at 280 and 320 nm. A shoulder appears at 250 nm at low temperature (77K). Two more bands are located at 225 and 200 nm. The last two bands are due to ligand to metal electron transfer, as is the band at 417 nm. The bands at 303 and 263 nm are due to metal to ligand electron transfer. There is disagreement over the assignment of the d to d transitions[28]. Ferrocyanide has bands at 422, 322, and 270 nm. These transitions are due to d to d excitations. There are bands at 218 and 200 which are metal to ligand charge transfer bands[29].

The mid-infrared has three absorptions for both potassium hexacyanoferrates. The frequencies for these stretches are listed in Table 1. The lower CN frequency in the ferrocyanide indicates that the extra electron partially occupies the Π^* orbitals of the cyanides.

Good values have been obtained for the redox potential of the half reaction:

$$[Fe(CN)_6]^{-3} + e^- \rightleftarrows [Fe(CN)_6]^{-4}$$

At an ionic strength of zero, the E^o is +.356 V. in aqueous solution at 25°C[30]. Studies of E^o over a range of temperatures have allowed the

Table 1. Infrared Frequencies for the Potassium Salts of the Hexacyanoferrates[26]

	$K_3Fe(CN)_6$	$K_4Fe(CN)_6*3H_2O$
C-N stretch	2110 cm^{-1}	2060 cm^{-1}
Fe-C-N deformation	510 cm^{-1}	526 cm^{-1}
Fe-C stretch	390 cm^{-1}	386 cm^{-1}

calculation of $\Delta H°$ of -111.8 kJ/mole and a value of $\Delta S°$ of -259 J/K*mole at 25°C. These values give a $\Delta G°$ of -189 kJ/mole[31].

Cobalt-phenanthroline Complexes

Blau first synthesized $Co(phen)_3Cl_3$ in 1898[32]. It is interesting that the first synthesis of 1,10-phenanthroline was reported in the same paper. Blau synthesized 1,10-phenanthroline in order to compare the properties of its metal complexes with those of bipyridine. This paper also described the synthesis of several other tris-phenanthroline metal complexes.

Stability constants for $Co(phen)_3^{+2}$ in aqueous solution are $\log K_1 = 7.0$, $\log K_2 = 6.7$, and $\log K_3 = 6.2$[33]. This follows the pattern for most other trisphenanathroline metal complexes.

Ligand exchange is generally a slow process for Co(III) complexes are fast for Co(II) complexes[34,35]. Co(III) $(phen)_3$ ligand exchange is catalyzed by the presence of Co(II) $(phen)_3$ complex through rapid electorn transfer[35]. The trisphenanthroline-cobalt(II) complex dissociates rapidly to the bisphenanthroline-diaquo and monophenanthroline-tetraaquo complexes in acidic media[36].

Infrared spectra of the $[Co(phen)_3]^{+2,+3}$ complexes are similar but distinguishable from each other[37]. A complete study of the electronic spectra has not been done. In the free form of phenanthroline, there are bands at 290, 264, and 223 nm[38]. These bands shift to the red when phenanthroline is coordinated to a metal[39]. Resolution of the two optical isomers of trisphenanthroline-cobalt(III) has been achieved[40].

Paglia and Sironi[41] have synthesized the all-cobalt analogs of the compounds which are the subject of this group's research. They have synthesized $Co_5(phen)_9(CN)_{12}*20H_2O$ and $Co_5(phen)_6(CN)_{12}*6H_2O$; the latter

being made from the former by washing with hot water. They have effective magnetic moments of 9.65 and 9.29 Bohr magnetons respectively. An effective magnetic moment of 9.94 would be consistent with nine unpaired electrons if we use a spin only approximation. This, in turn, indicates the presence of three high-spin Co(II) atoms and two low spin Co(III) atoms per formula unit.

In a related work, Salvedeo[42] reports the synthesis of $[Fe(phen)_3]_3[Co(CN)_6]_2*11H_2O$ and of $K[Fe(phen)_3][Co(CN)_6]*4.5H_2O$, which are metal-exchange isomers of the compounds of interest to us.

Preparation of Compounds

a) $K_3Fe(CN)_6$ and $K_4Fe(CN)_6*3H_2O$ were recrystallized from commercial samples.

b) $Co(phen)_3Cl_2$ was prepared by placing approximately one gram of $CoCl_2*6H_2O$ in twenty milliliters of water. Nitrogen was bubbled through the solution to remove dissolved oxygen. The temperature was raised to about 90°C and then three equivalents of 1,10-phenanthroline monohydrate were added. The resulting solution was allowed to react for forty-five minutes at 90°C. The solution was cooled to room temperature and a saturated aqueous solution of NaCl was added to precipitate $Co(phen)_3Cl_2$. The resulting golden-yellow precipitate was recrystallized from a 50/50 acetone-water solution.

c) $Co(phen)_3(ClO_4)_3*2H_2O$ was prepared according to the method of Schilt and Taylor[34].

d) $Co(phen)_2Cl_2$ was prepared by letting a solution of 5 grams of $Co(phen)_3Cl_2$ in 50 milliliters of DMSO stand for about forty-five minutes, at which time fairly large red crystals form. The precipitate was recrystallized from acetone to which a small amount of water had been added. The recrystallized compound is pink in color. This preparation is an improvement over the previous preparations in the literature as it takes only a few hours and produces an anhydrous product[35]. The monohydrate can be formed by using a higher water/acetone ratio when recrystallizing.

e) $[Co(phen)_2]_3[Fe(CN)_6]_2*23H_2O$, (for brevity labeled (I*A) from here on), was prepared by dissolving 3.1 grams of $Co(phen)_3Cl_2$ in 25 ml of water. It is important that the water be deionized and distilled; the reaction generally went awry using the distilled water from the "tap". Nitrogen was

bubbled through the solution and the temperature raised to 80°C. 1.7 grams of potassium ferricyanide were dissolved in 7 ml of deoxygenated water and this was added to the first solution. A fine green precipitate formed immediately. The precipitate was then dried in vacuo at 100°C over phosphorus pentoxide. The color at this point is variable (brown or green).

The sample is most likely $[Co(phen)_3]_3[Fe(CN)_6]_2$ with some smaller amount of $[Co(phen)_2]_3[Fe(CN)_6]_2$ mixed in. When the compound is dried, it may or may not turn brown in color. When examined under the microscope, yellow crystals are seen mixed with the green or brown.

The dried precipitate, regardless of color, was placed in approximately 50 ml of DMSO at 60°C under dry nitrogen and stirred for two hours. It is important for the precipitate to have been dried, otherwise the surface water which is carried in with it will prevent it from going into solution. Similarly, DMSO which had been allowed to absorb H_2O from the atmosphere also would not dissolve the precipitate. The solution turned brown as the compound (brown or green form) dissolved. Furthermore the sample which remained undissolved turned brown within ten minutes after being placed in the DMSO, if it was not so already. (If it does not, it indicates that the DMSO is wet.) The portion which did not dissolve was filtered off and the solution allowed to cool. Dry acetone was added to the solution until a reddish brown precipitate formed. This was filtered off and dried in vacuo at 100°C over phosphorus pentoxide. The presence of a strong SO stretch band in the infrared spectrum indicates that the resulting compound contains DMSO in the lattice. The DMSO can be removed by washing several times with water to achieve a pure (green) product.

The resulting compound is dark green in the hydrated form (I*A) and reddish-brown in the anhydrous form (I). A reasonably pure sample will

interconvert between the two forms easily as it absorbs atmospheric water rapidly; the anhydrous form will become fully hydrated in a few minutes if the compound is spread out. It will dehydrate under vacuum or at about 60°C in the open atmosphere. Compounds I and I*A are soluble only in DMSO. The color is somewhat lighter green when the crystals are wet than when dry but not dehydrated. The solid texture is very fine, like clay, making the compound very difficult to purify, as it clogs frits and must be washed many times to remove impurities.

As mentioned above, the precipitate which is originally obtained from the reaction in water is poorly characterized but appears to be a mixture of I*A and the analogous trisphenanthroline-cobalt salt, the comound which was originally sought. When the precipitate is dried, it may or may not change color. In any case the conditions required to cause the color change are more extreme than those for pure (I*A). Compound I was chosen for the study as it was possible to obtain it in pure form, while a method for preparing $[Co(phen)_3]_3[Fe(CN)_6]_2$ has not yet been devised.

f) Two alternate methods have been devised for the synthesis of $Co_3Fe_2(phen)_6(CN)_{12}*23H_2O$. Instead of mixing the trisphenanthroline-cobalt salt with the ferricyanide, the bisphenthroline-cobalt salt can be prepared as above and used in its place. This method avoids the formation of the yellow solid in the initial precipitate. The other method involves using a diffusion apparatus which has three chambers separated by medium glass frits. A concentrated solution of bisphenanthroline-cobalt dichloride in DMSO is placed in one end chamber. A concentrated solution of potassium ferricyanide in DMSO is placed in the other end chamber. The middle chamber contains DMSO with 10% acetone. This is allowed to sit for aweek. I forms in the middle chamber. This method produces a superior product in that it

Table 2. Chemical Analysis of $[Co(phen)_3]_3[Fe(CN)_6]_2 \cdot 23H_2O$

	%Co	%Fe	%C	%H	%N	%O
Analysis	8.68	5.20	49.79	2.72	16.38	17.23*
Theoretical	8.60	5.43	49.12	4.41	16.36	16.08

* The value for oxygen the analysis was calculated by mass balance.

is relatively pure when first synthesized; but without improvement in crystal quality. However, it takes a long time and the glassware is difficult to clean.

Elemental analyses of I*A were performed by Galbreath Labs[43]. The hydrated form was analyzed for iron, cobalt, carbon, hydrogen, and nitrogen. The results are tabulated in Table 2 where the theoretical values are for an empirical formula of $C_{84}Co_3Fe_2H_{94}N_{24}O_{23}$, corresponding to $[Co(phen)_2]_3[Fe(Cn)_6]_2*23H_2O$. Thermogravimetric analysis gave a value of 18.11% H_2O for room temperature sample (see next section). This was the value used for the weight of the water in calculating the theoretical elemental compositions. These values are in good agreement with the analyses, except for hydrogen which is in error by 1.7%.

Instrumental Methods

Electron spin resonance spectra were collected on a Bruker Model ER 200D-SRC using an X-band microwave bridge and a rectangular cavity. All spectra were taken at room temperature using microcrystalline samples.

Magnetic susceptibility measurements and thermogravimetric analyses were done on a Cahn/Ventron Faraday Balance employing a Cahn Electrobalance DTL. Temperature measurements were made using a pair of copper-constantan thermocouples referenced to 273.15K using an ice-water bath. The emf difference of the thermocouples was measured with a Honewell Model 2704 Portable Potentiometer. Room temperature measurements of water sensitive samples were made by sealing the samples in a borosilicate (pyrex) glass ampule to which a small glass hook had been attached.

Mossbauer spectra were collected with a locally constructed computer-based instrument operating in the constant acceleration mode[3]. The source

used was 10 mCu ^{57}Co in a palladium matrix. The Doppler velocity scale was calibrated with an enriched ^{57}Fe foil absorber. A single sample was prepared placing the compound between a sheet of plastic and 3M tape. Once mounted in the cryostat cold finger, this one sample could be hydrated or dehydrated, as was necessary, as water readily passes through the 3M tape. Anhydrous samples were kept anhydrous by assembling the cold finger mount in the cryostat vacuum chamber.

Samples for infrared spectra were prepared as Nujol mulls on potassium bromide plates. Spectra were collected on a Perkin Elmer 1330 Infrared Spectrometer. The wavenumber scale was calibrated with a polystyrene film. Samples of I were prepared in a glove box to minimize contact with atmospheric water. Samples did not appear to hydrate significantly in the period during which the spectrum was recorded.

Ultraviolet and visible spectra were taken on a Cary Recording Spectrophotometer Model 11. Solution samples used water or DMSO as the solvent. Solid samples were ground and suspended in an 0.5 weight per cent agar gel. The agar/water mixture was heated on a hot plate until the agar dissolved and then the solution was allowed to cool. The solution thickens as it cools. A small amount of the compound to be studied was placed in the solution before it gelled. The solution was stirred manually to achieve a uniform distribution of sample in the gel. The solution was then placed in a cuvette and allowed to solidify. A similar technique was used for I*A in DMSO. This suspension will not gel, but the viscosity is high enough to prevent settling of the solid.

Results

Thermogravimetric Analysis and Variable Temperature Magnetic Susceptibility. These two experiments were run simultaneously as the results of the variable temperature magnetic susceptibility measurements are dependent upon the weight loss of water as the temperature is raised.

The amount of water in the lattice of compound I*A is dependent on the temperature. The temperature was raised gradually over a period of eight hours in order to make sure the comopund was in equilibrium with the atmospheric water. Thermogravimetric analysis showed that the compound is nearly completely hydrated at 289K and was completely dehydrated at 333K (see Figure 1). Knowing one can dehydrate the compound in a vacuum at room temperature, the hydration of the lattice is dependent upon the relative humidity of the laboratory. It is assumed that the humidity in the lab (not measured) was relatively constant over the course of the experiment. From the sample weight loss to constant mass, it has been determined that there are twenty-three waters per formula unit of I*A.

The effect of the changing water content on the mass and diamagnetic susceptibility of the sample with temperature had to be compensated for in computing X_M from the magnetic susceptibility data. X_g was first calculated in the usual way[44]. The mass of water left in the sample was multiplied by $X_g(H_2P)$ and subtracted from the raw X_g data to obtain X_g for the sample as if it were anhydrous at all temperatures. From these values X_{para} and U_{eff} were obtained for each temperature (Figures 2 and 3). These figures show that a cooperative spin transition occurs between 306K and 312K. The high temperature value of U_{eff} is 9.0 and the low temperature value is 6.38. (These correspond to 8 and 5 unpaired electrons in the compound).

Figure 1. Thermogravimetric Analysis of $[Co(phen)_2]_3[Fe(CN)_6]_2$

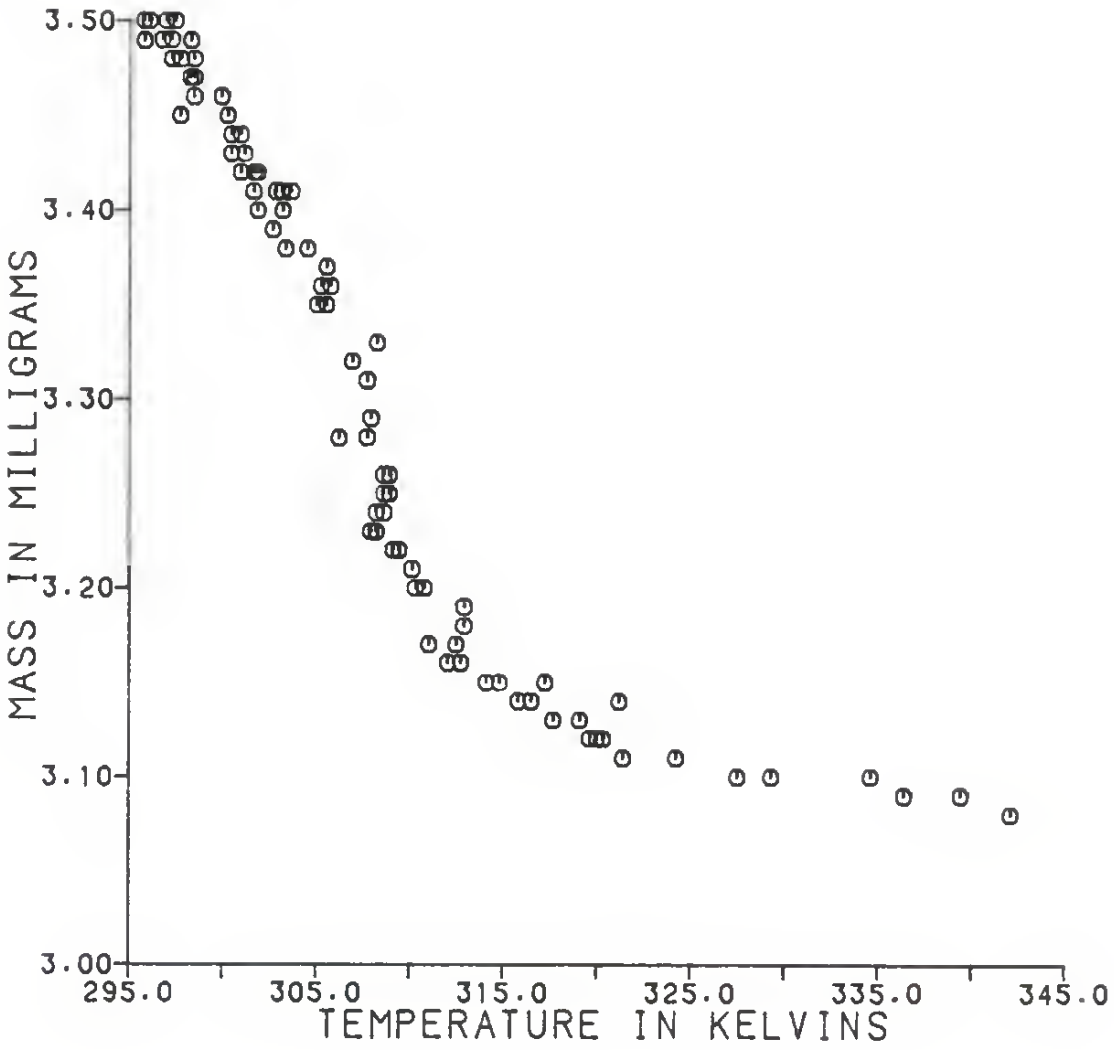
3.50
3.40
3.30
3.20
3.10
3.00
MASS IN MILLIGRAMS
295.0
305.0
315.0
325.0
335.0
345.0
TEMPERATURE IN KELVINS

Figure 2. Effect of Temperature on the Paramagnetic Susceptibility of $[Co(phen)_2]_3[Fe(CN)_6]_2$

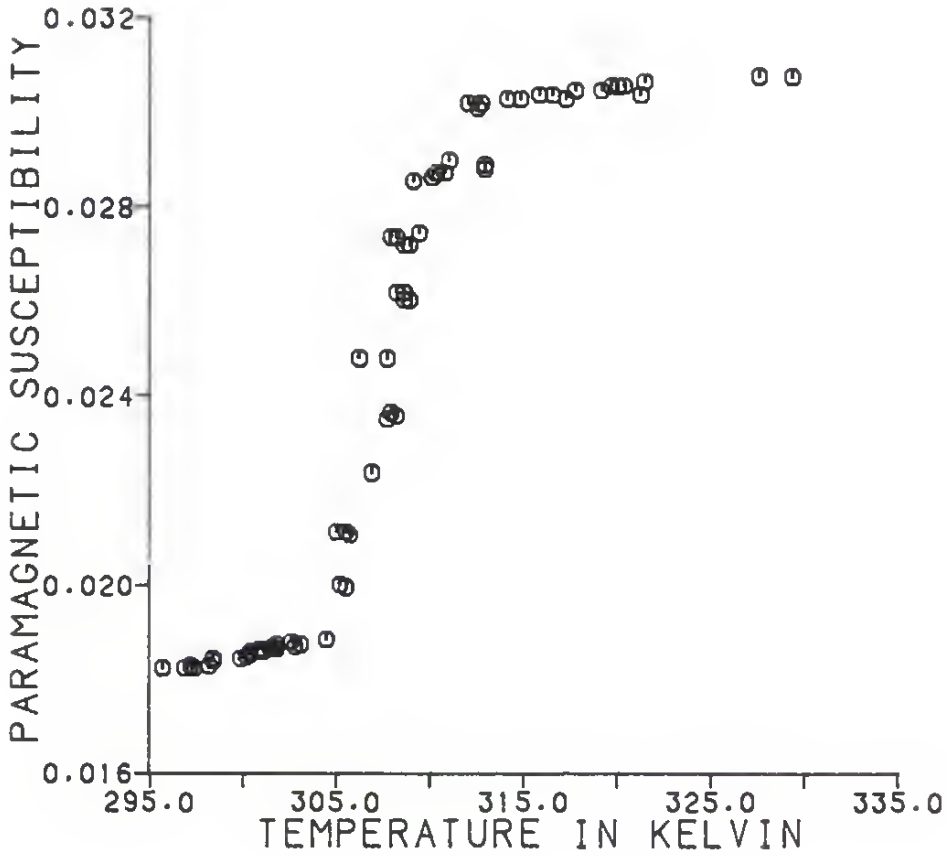
PARAMAGNETIC SUSCEPTIBILITY
0.032
0.028
0.024
0.020
0.016
295.0
305.0
315.0
325.0
335.0
TEMPERATURE IN KELVIN

Figure 3. Effective Magnetic Moment of $[Co(phen)_2]_3[Fe(CN)_6]_2$ Versus Temperature

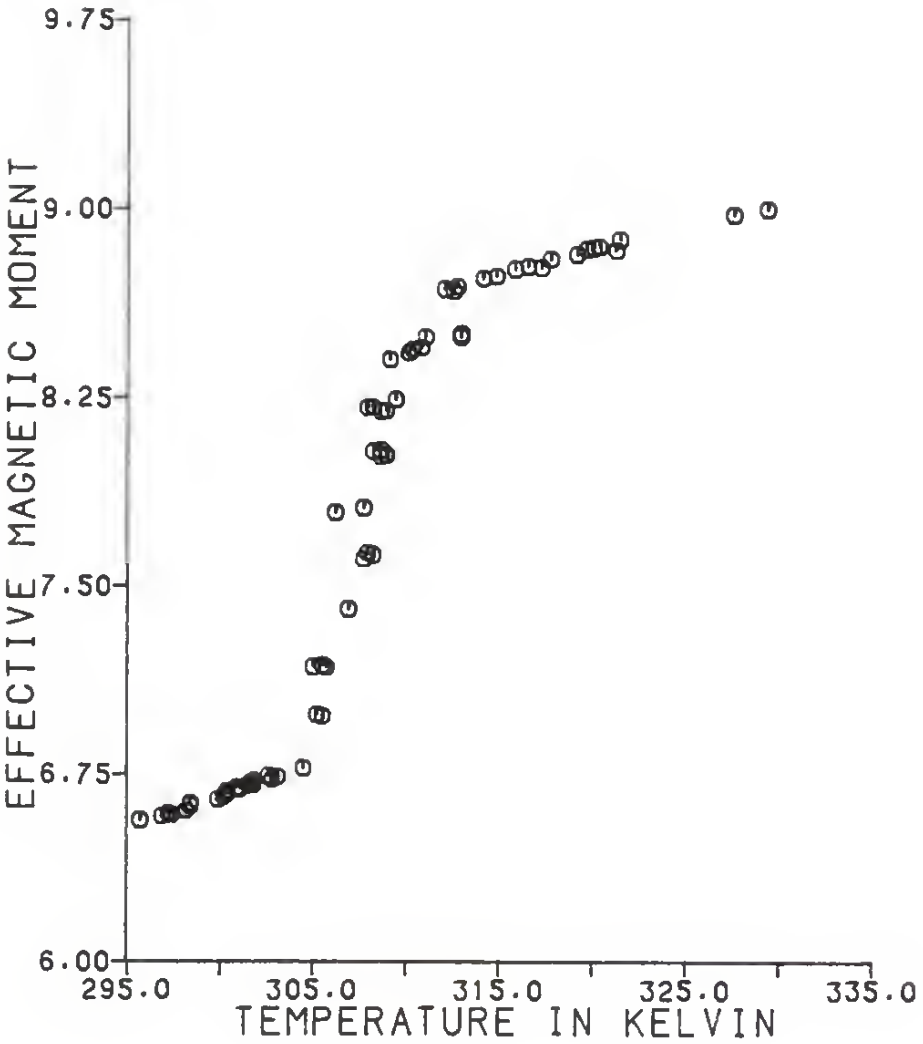
9.75
9.00
8.25
7.50
6.75
6.00
EFFECTIVE MAGNETIC MOMENT
295.0
305.0
315.0
325.0
335.0
TEMPERATURE IN KELVIN

In order to determine whether the spin transition is caused solely by the increase in temperature or requires the loss of water, magnetic susceptibility measurements were made on a sample of the anhydrous form. X_{para} for the anhydrous form at 295K is $3.37 * 10^{-2} \pm 1.0 * 10^{-4}$ cgs units, which corresponds to a U_{eff} of 8.92 ± 0.12. This indicates that the spin state is dependent upon the extent of hydration and not on the temperature.

Infrared Spectroscopy. The infrared spectrum of (I) is similar to that of the compound $Co(phen)_2Cl_2$ (see Table 3). This is not surprising since most of the bands are due to the phenanthroline vibrations. The interesting features of the infrared are found in the absorptions due to cyanide. The single broad band with high energy shoulders seen in the CN stretch region of the hydrated form is split into three bands in the anhydrous form (Figure 4.), all three at slightly higher frequency than their counterparts in the hydrated compound. The weak broad band at 2055 cm^{-1} in I is suspiciously similar in appearance to the 2045 cm^{-1} band in I*A. The weak band at 548 cm^{-1} in I*A is most likely due to Fe-C-N deformation. The broad band at 3325 cm^{-1} in the hydrated sample is due to water in the lattice.

Visible Spectroscopy. Because I*A is not soluble in water, its visible spectrum was obtained from a sample suspended in agar gel. While this technique allows one to obtain a spectrum which would not otherwise be available, it precludes quantitative results. For comparison, the visible spectra of potassium ferrocyanide, potassium ferricyanide, trisphenanthroline-cobalt(II) perchlorate, trisphenanthroline-cobalt(III) perchlorate, trisphenanthroline-cobalt(II) chloride and bisphenanthroline-cobalt(II) dichloride (not shown) were made. The spectrum of (I) appears to

Table 3.
Comparison of Infrared Frequencies of $Co(phen)_2Cl_2$ and The Hydrated and Anhydrous Forms of $[Co(phen)_2]_3[Fe(CN)_6]_2$

$Co(phen)_2Cl_2$	$[Co(phen)_2]_3[Fe(CN)_6]_2$	
	anhydrous form (I)	hydrated form (I*A)
409m	410m	
431w	427w	432w
	452w	452w
468w	482w	485w
490w	497w	497w
501w		
533w	535w	535m
625m		
	629m	629w
	645w	645w
715st	715st	715st
	739w	735w
764m	761m	759m
837st	835st	835st
852st	854m,si	852w,si
	868w	868w
926w		
1031w	1025w	1025w
1072m,si	1077si	1080br
1086m	1089m	
1126m	1128m	1128m
1135m		
1292m	1197si	1194si
1203m	1210m	1210w
1285w	1295w	1289w
1325m	1327m	1327m
1403st	1407st	1409st
1477m	1479m	1479m
1492m	1497m	1499m
1521w,si	1542w,si	1542w,si
1557m	1563m	1563m
1603m,br	1607m,br	1607m,br
	2055m,br	2045st,br
	2095st	2085st,si
	2120m	2115m,si
		3315br

br - broad m - medium si - sideband
st - strong w - weak

Figure 4. Infrared Spectra of the CN Stretching Bands of $[Co(phen)_2]_3[Fe(CN)_6]_2$

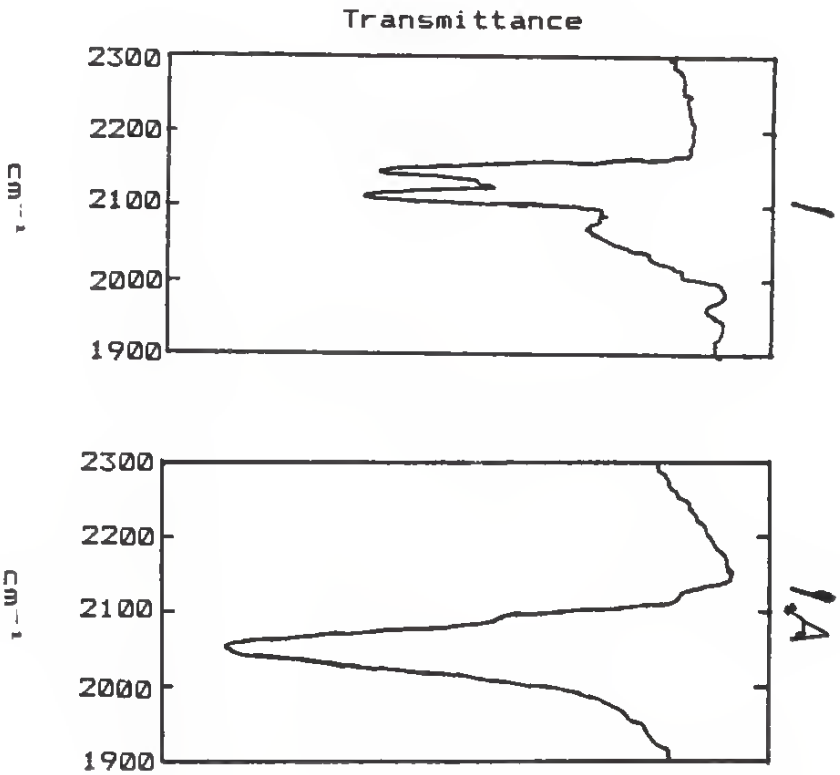
Transmittance
2300
2200
2100
2000
1900
cm⁻¹
1
2300
2200
2100
2000
1900
cm⁻¹
1A

be the superposition of the spectra for $[Co(phen)_2Cl_2]^{+2}$ and $\{Fe(CN)_6]^{+3}$ solutions in DMSO (Figures 5, 6 and 7). The band at 320 nm in the Ferricyanide spectra is an artifact which only occurs when the sample is run in DMSO. The Co center is probably in solution as $[Co(phen)_2(DMSO)2]^{+2}$. In I*A, extra bands appear at 520 and 650 nm (Figure 8). These bands are the cause of the greencolor in the hydrated compound. These bands were not detected in the anhydrous form, even in the near-infrared region (1250nm - 640nm). The wavelength of the absorption maxima for all four species are tabulated in Table 4. Unfortunately, useful data could not be obtained in the ultra-violet region due to the absorption of ultraviolet light both by DMSO and agar.

Electron Paramagnetic Resonance Spectroscopy. $[Co(phen)_2]_3[Fe(CN)6]_2$ has an X-band epr spectrum which is independent of the extent of hydration (Figures 9 and 10) $Co(phen)_2Cl_2$ gives a very weak spectrum (Figure 11), the intensity of the potassium ferricyanide spectrum is about 100 times as strong (Figure 12). Potassium ferricyanide gives a spectrum with peaks at g = 2.26 and .776. (Figure 12). The spectra for both forms of (I) are similar to the potassium ferricyanide spectrum. Failure to observe the Co^{2+} is not surprising considering the intensity of the signal from the $Co(phen)_2Cl_2$. The fine structure found in the ferricyanide spectrum is blurred out in the spectra of I and I*A.

Mossbauer Spectroscopy. ^{57}Fe spectra for both hydrated and anhydrous forms were taken over a range of temperatures from 77K (liq. N_2) up to room temperature. The hydrated form (Figures 13-15) exhibits a single line, while the anhydrous form (Figures 17-19) shows an extremely weak doublet,

Figure 5. Visible Spectrum of $Co(phen)_2Cl_2$

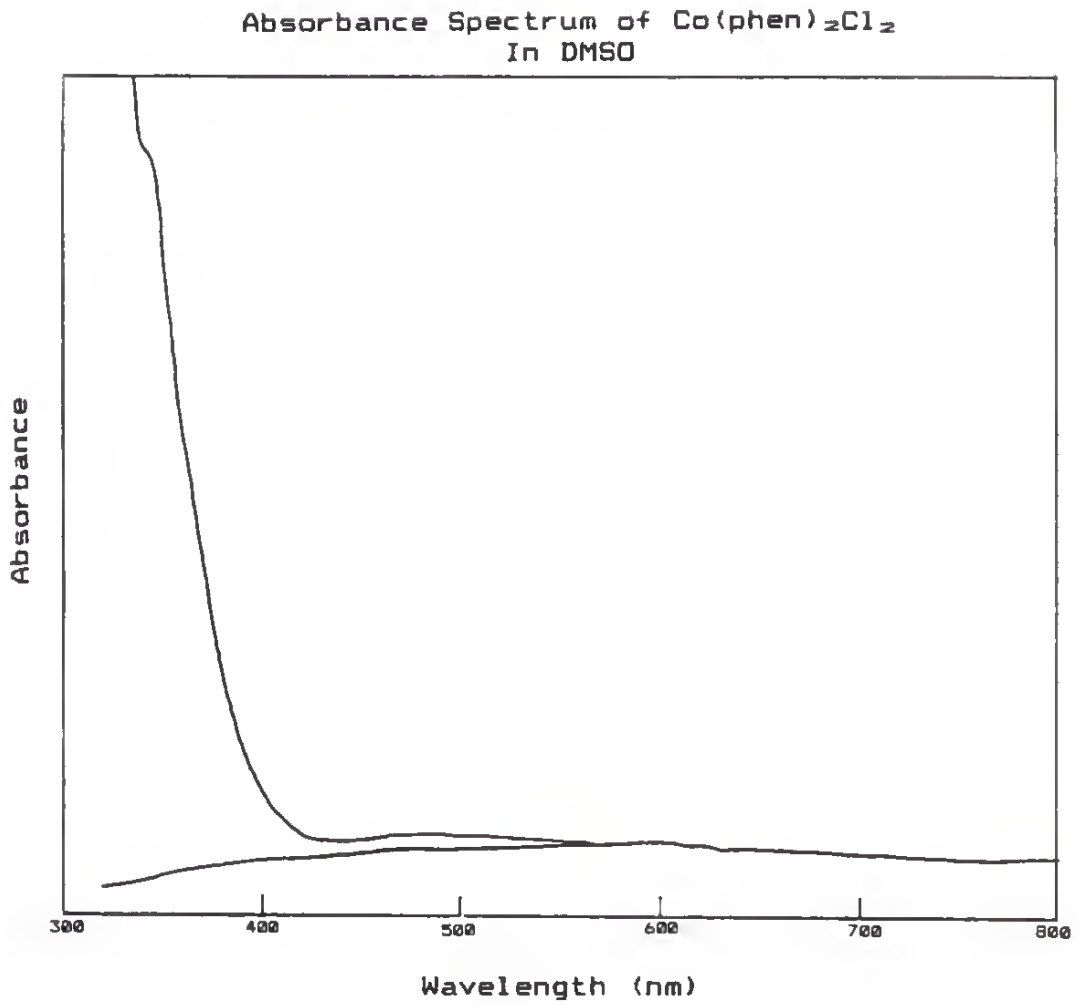
Absorbance Spectrum of Co(phen)₂Cl₂
In DMSO
Absorbance
300
400
500
600
700
800
Wavelength (nm)

Figure 6. Visible Spectrum of $K_3Fe(CN)_6$

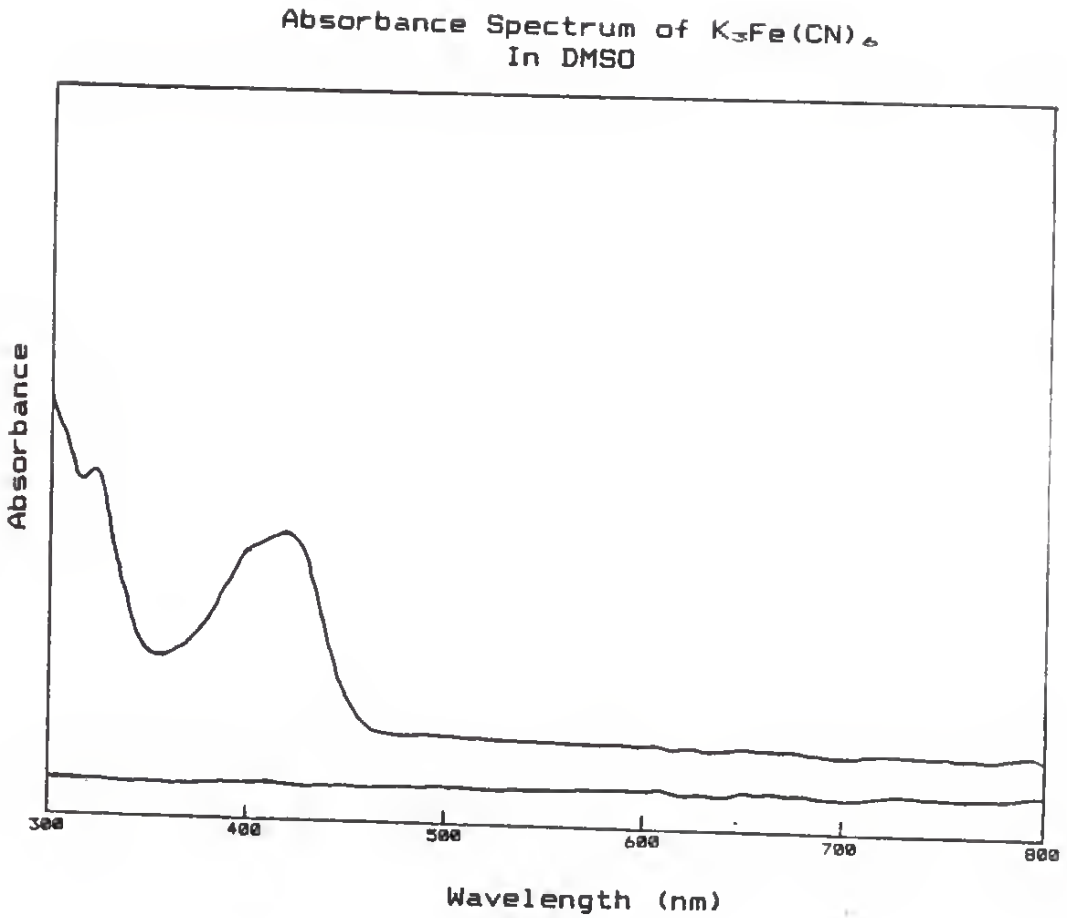
Absorbance Spectrum of $K_3Fe(CN)_6$
In DMSO
Absorbance
300
400
500
600
700
800
Wavelength (nm)

Figure 7. Visible Spectrum of $[Co(phen)_2]_3[Fe(CN)_6]_2$

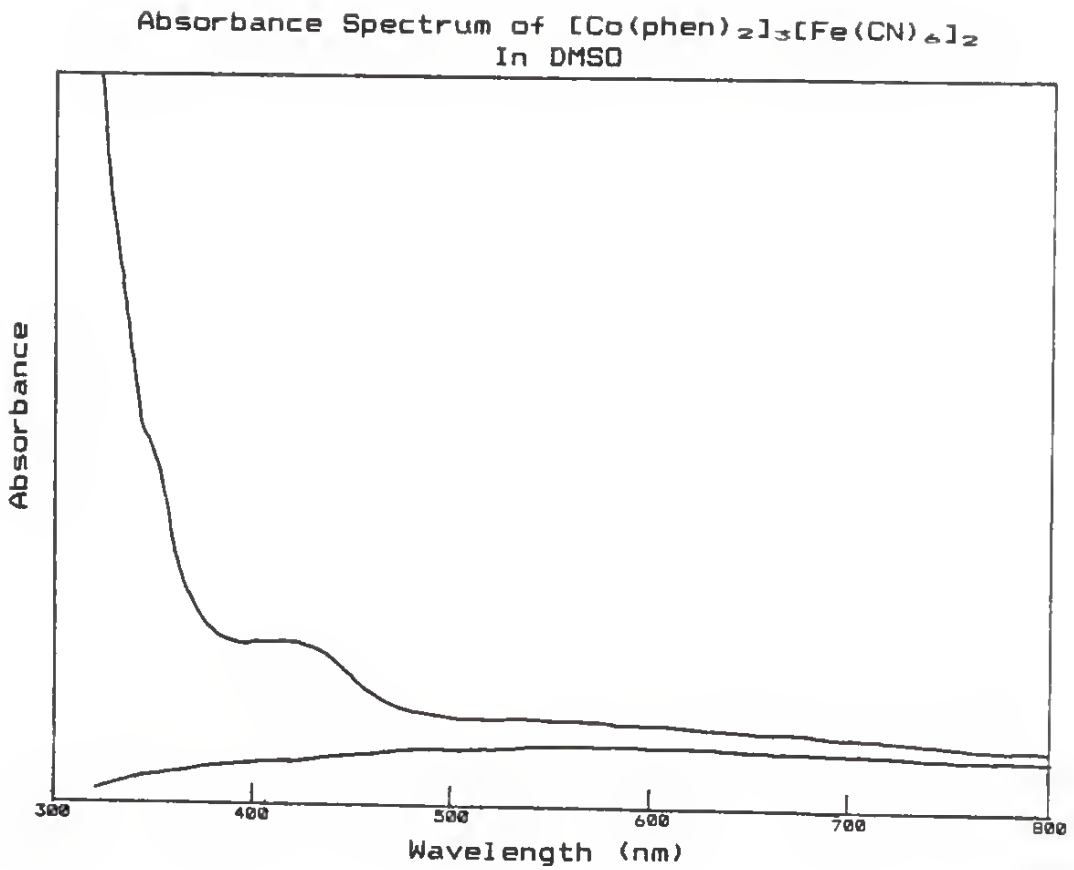
Absorbance Spectrum of [Co(phen)2]3[Fe(CN)6]2
In DMSO
Absorbance
300
400
500
600
700
800
Wavelength (nm)

Figure 8. Visible Spectrum of $[Co(phen)_2]_3[Fe(CN)_6]_2*23H_2O$

Absorbance Spectrum of $[Co(phen)_2]_3[Fe(CN)_6]_2*23H_2O$
In an Agar-Water Suspension

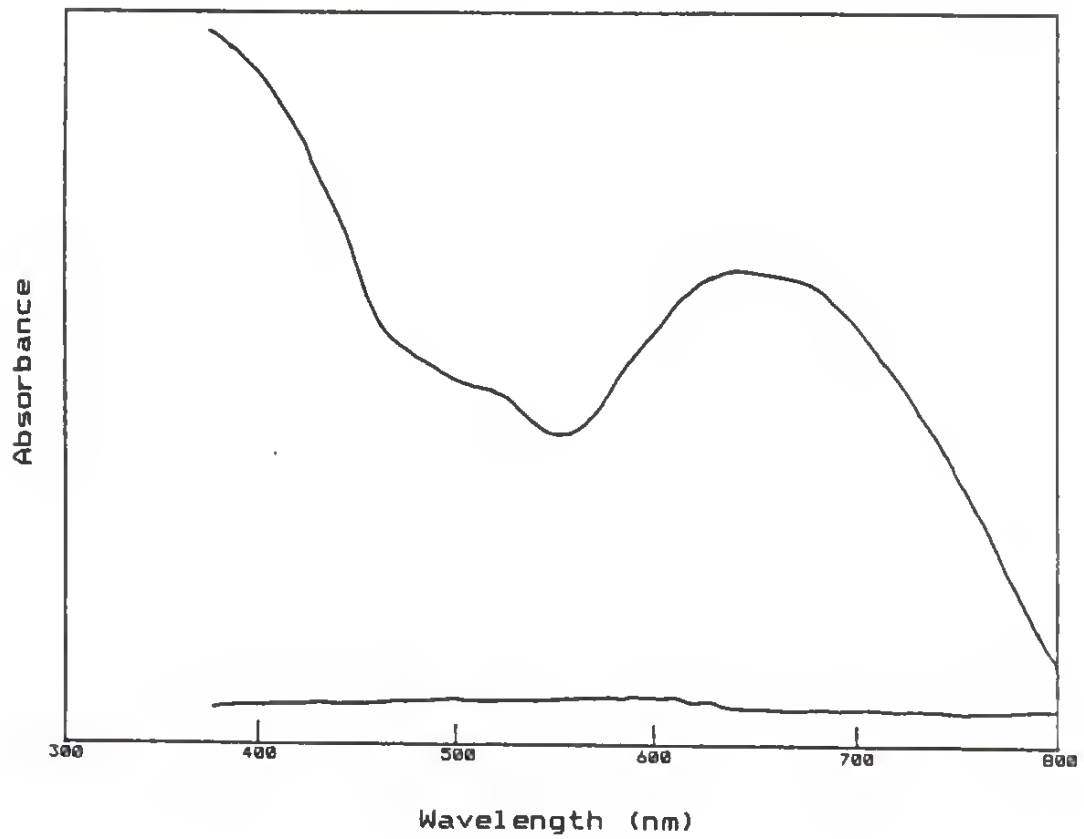

Table 4.
Comparison of the Electronic Band Positions (nm) of $[Co(phen)_2]_3[Fe(CN)_6]_2$ With Those of It's Constituent Ions

$Co(phen)_2Cl_2$ (in DMSO)	$K_3Fe(CN)_6$ (in DMSO)	$[Co(phen)_2]_3[Fe(CN)_6]_2$ anhydrous (in DMSO)	$[Co(phen)_2]_3[Fe(CN)_6]_2$ hydrated (agar gel)
345sh		345sh	345br
	400sh		
	420	420br	
			520sh
			650nm

br - broad sh - shoulder

Figure 9. Electron Paramagnetic Resonance Spectrum of $[Co(phen)_2]_3[Fe(CN)_6]_2$

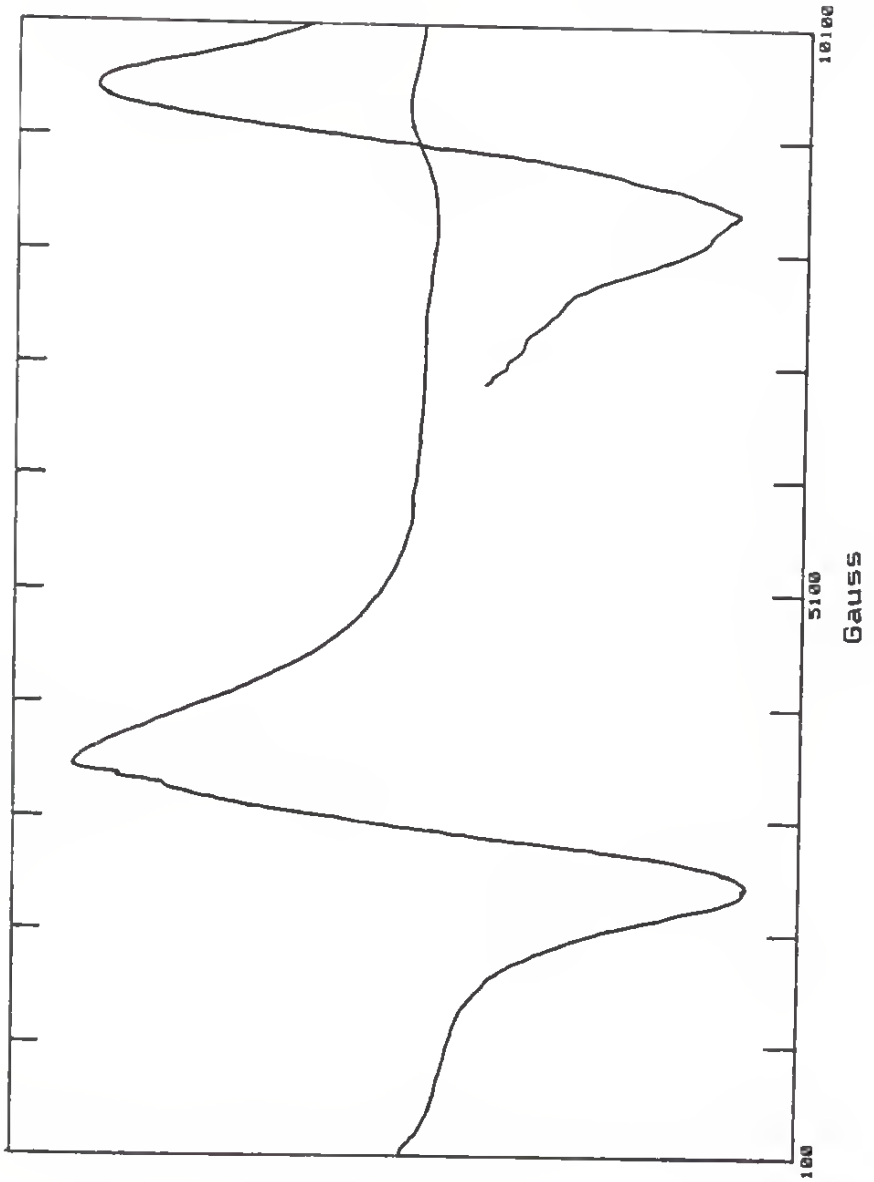
10100
5100
100
Gauss

Figure 10. Electron Paramagnetic Resonance Spectrum of $[Co(phen)_2]_3[Fe(CN)_6]_2*23H_2O$

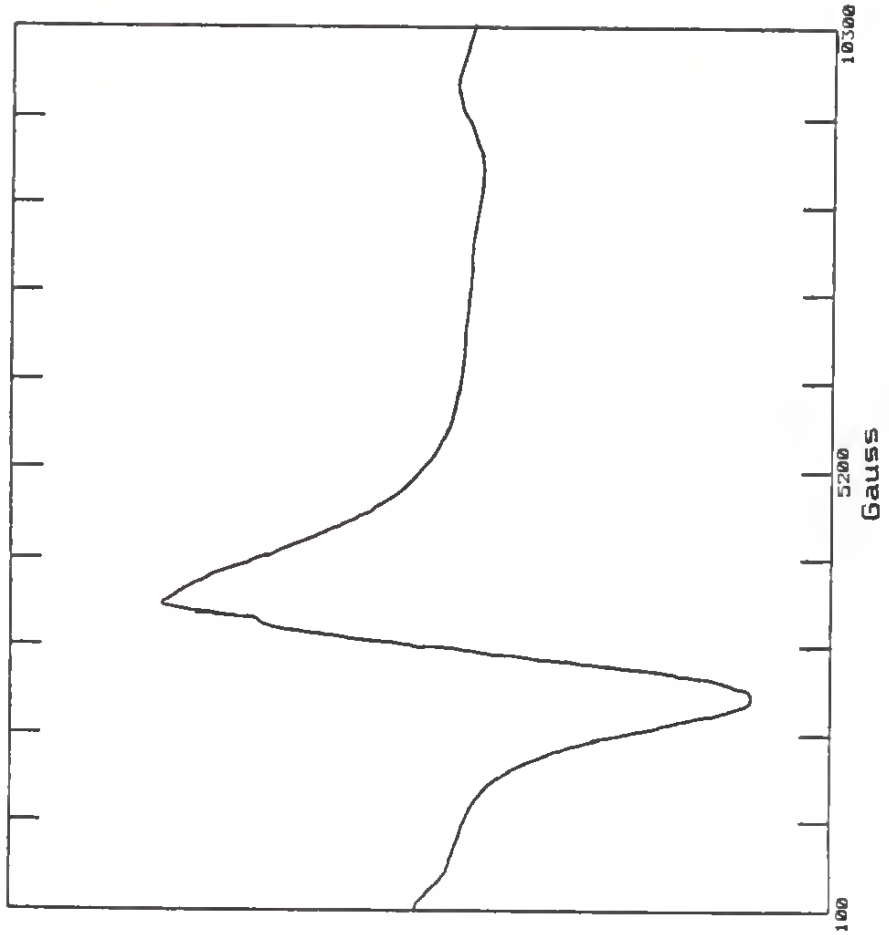
10300
5200
Gauss
100

Figure 11. Electron Paramagnetic Resonance Spectrum of $[Co(phen)_2]Cl_2$

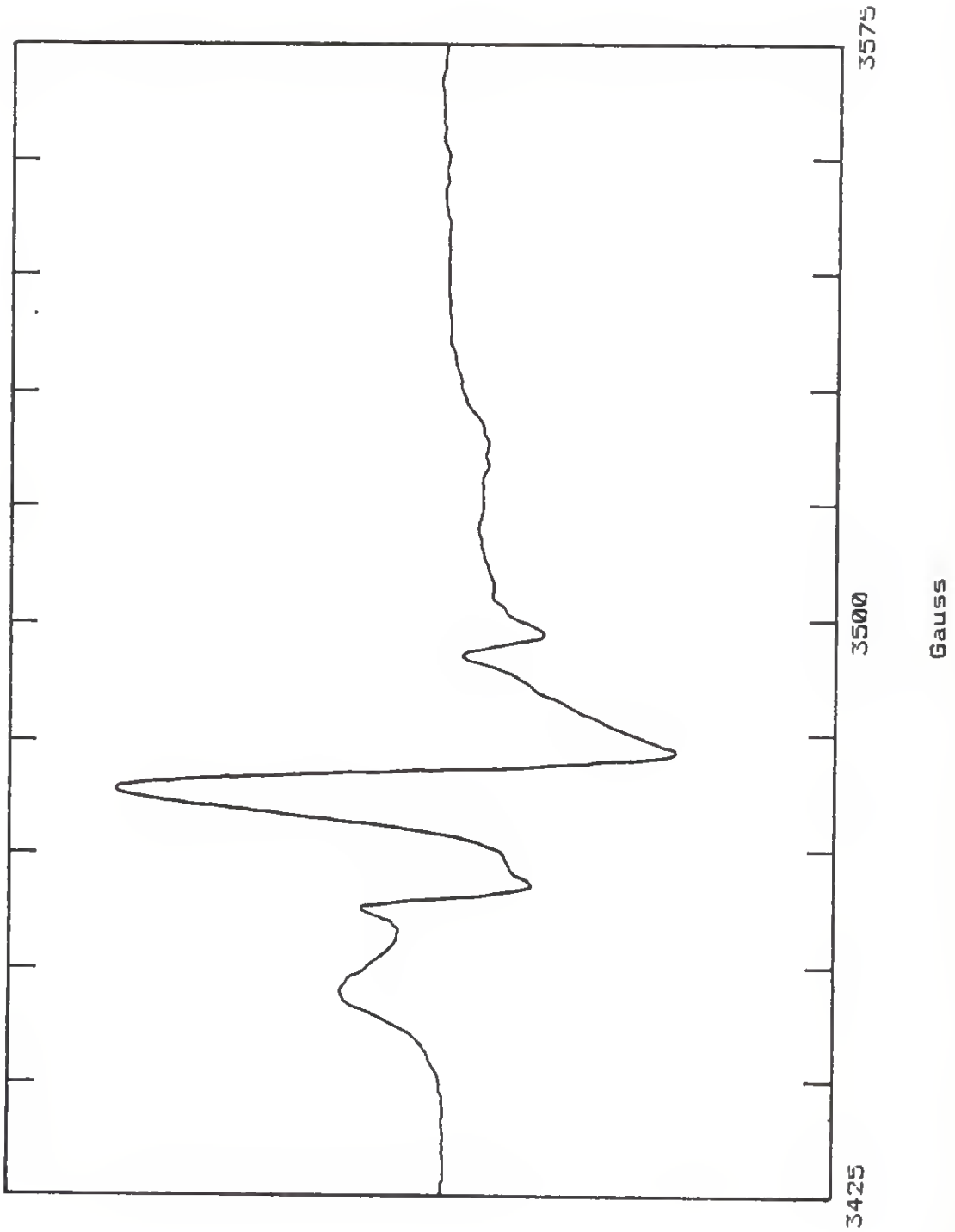
3575
3500
3425
Gauss

Figure 12. Electron Paramagnetic Resonance Spectrum of $K_3Fe(CN)_6$

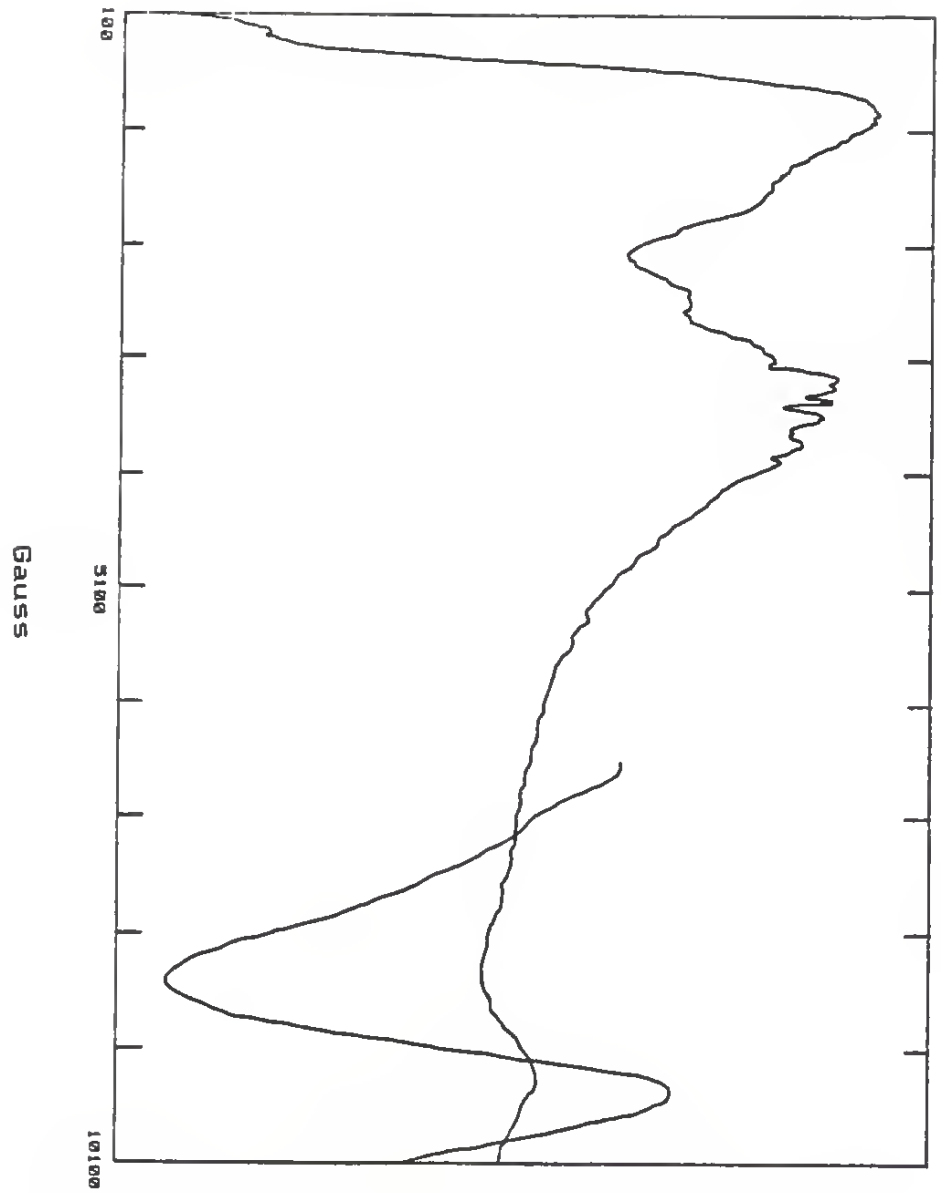
Gauss
100
5100
10100

Figure 13. Mossbauer Spectrum of $[Co(phen)_2]_3[Fe(CN)_6]_2*23H_2O$ at 77K

MOSSBAUER SPECTRUM OF
[CO(PHEN)2]3[FE(CN)6]2*23H2O, 77K
COUNTS =228748.

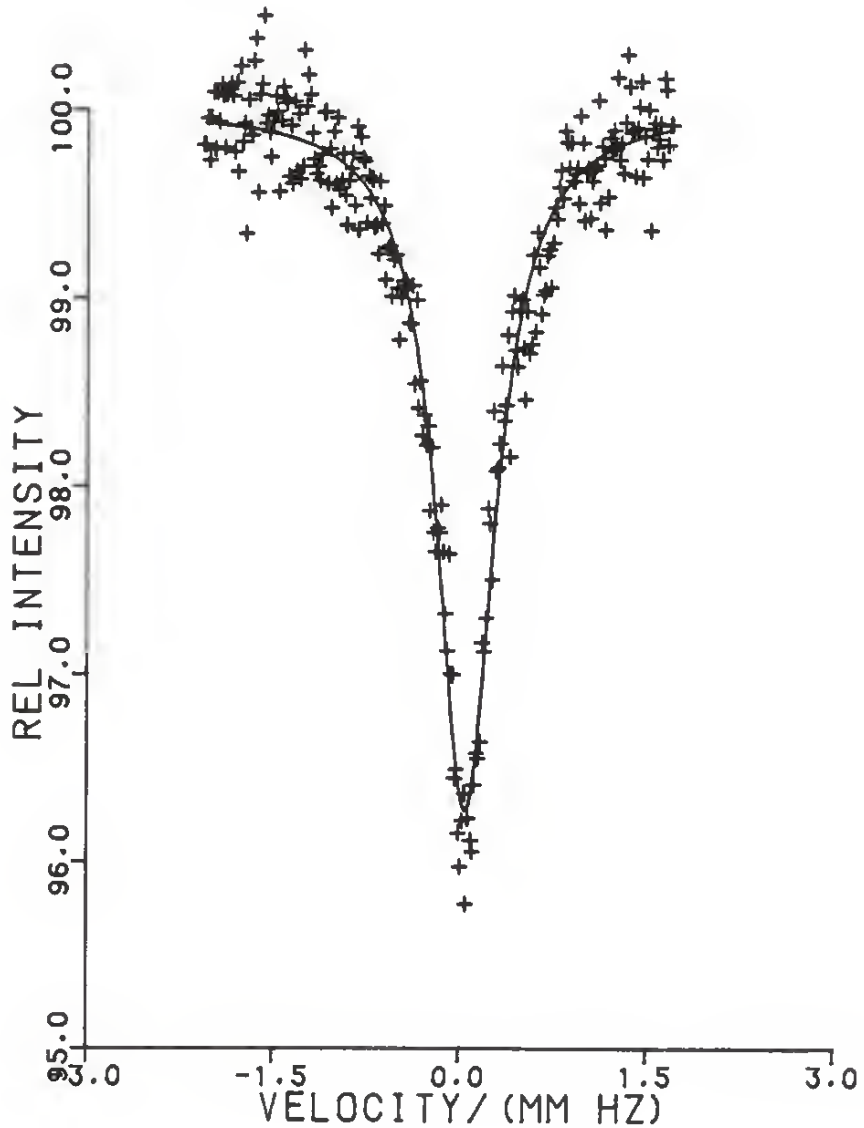

Figure 14. Mossbauer Spectrum of $[Co(phen)_2]_3[Fe(CN)_6]_2*23H_2O$ at 195K

MOSSBAUER SPECTRUM OF
[CO(PHEN)2]3[FE(CN)6]2*23H2O, 195K
COUNTS =308899.

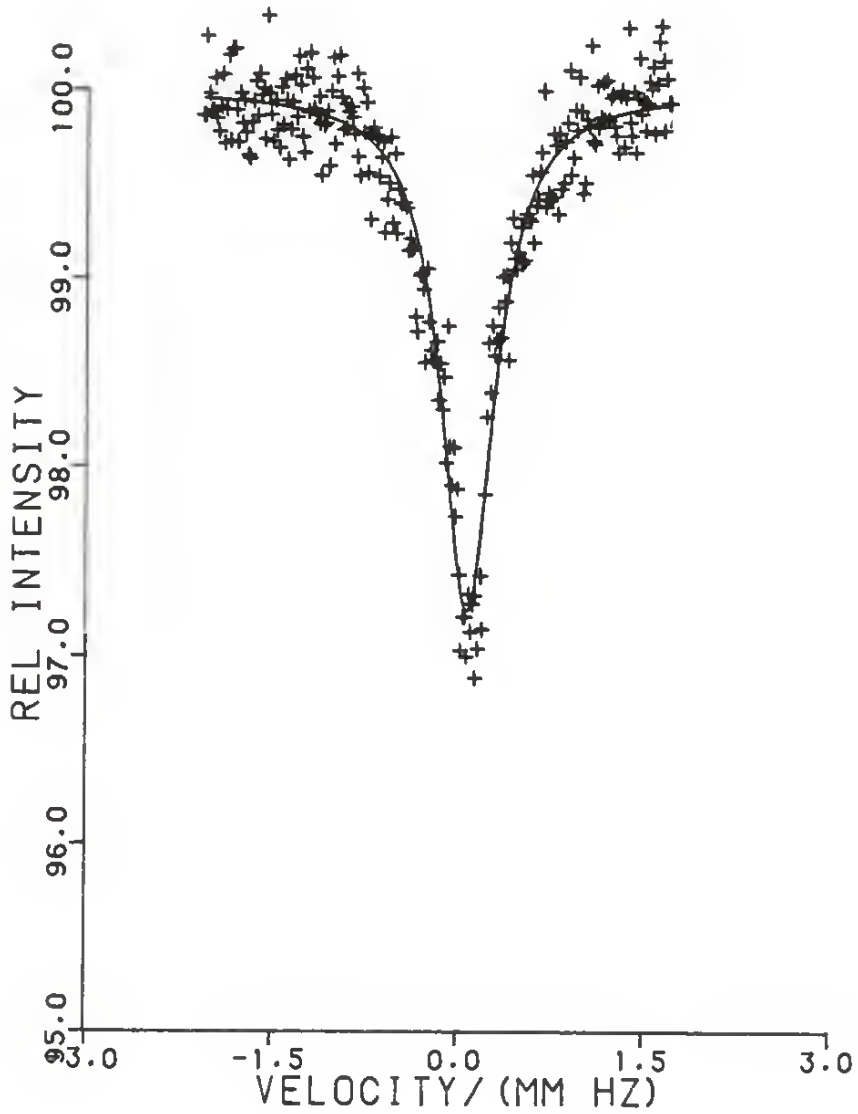

Figure 15. Mossbauer Spectrum of $[Co(phen)_2]_3[Fe(CN)_6]_2*23H_2O$ at 275K

MOSSBAUER SPECTRUM OF
[CO(PHEN)2]3[FE(CN)6]2*23H2O, 275K
COUNTS =400841.

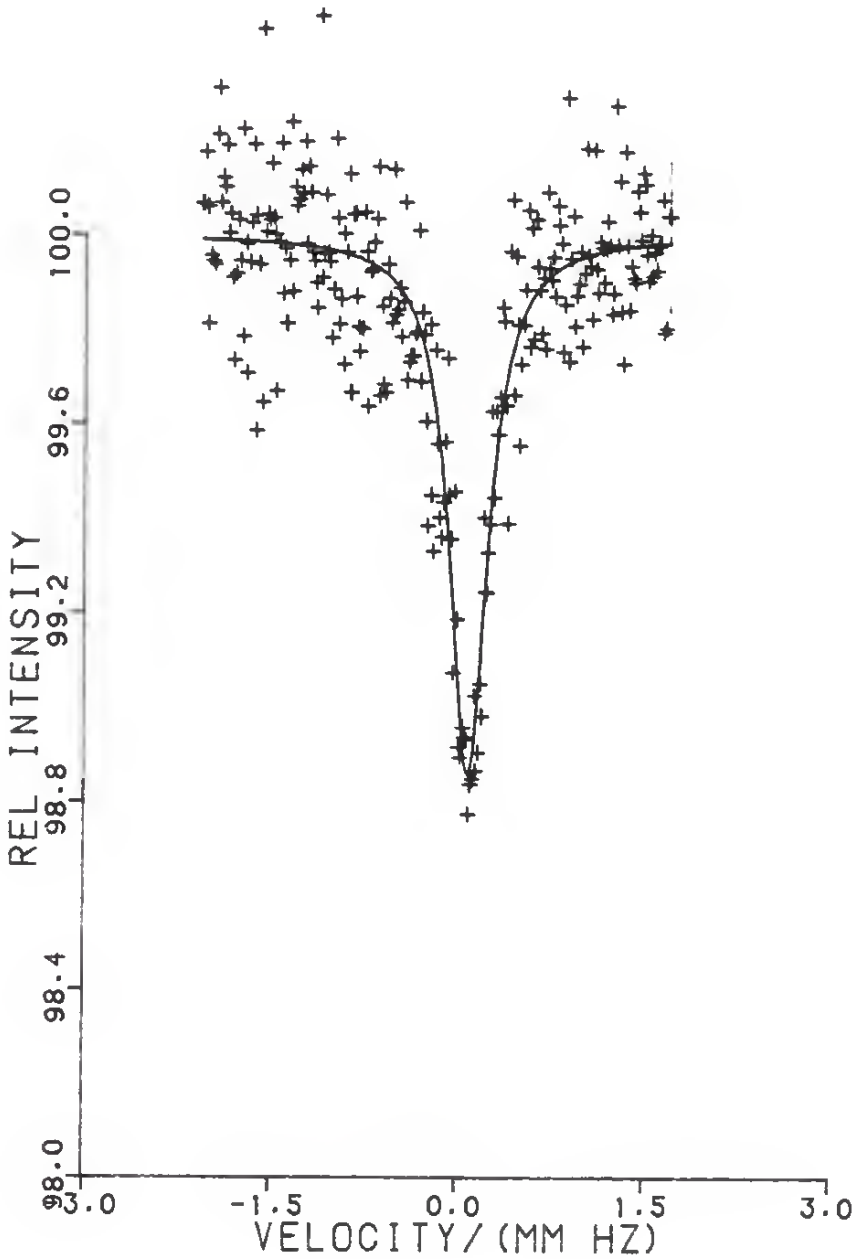

Figure 16.] Mossbauer Spectrum of

$[Co(phen)_2]_3[Fe(CN)_6]_2*23H_2O$ at 295K

MOSSBAUER SPECTRUM OF
[CO(PHEN)2]3[FE(CN)6]2*23H2O, 295K
COUNTS =522199.

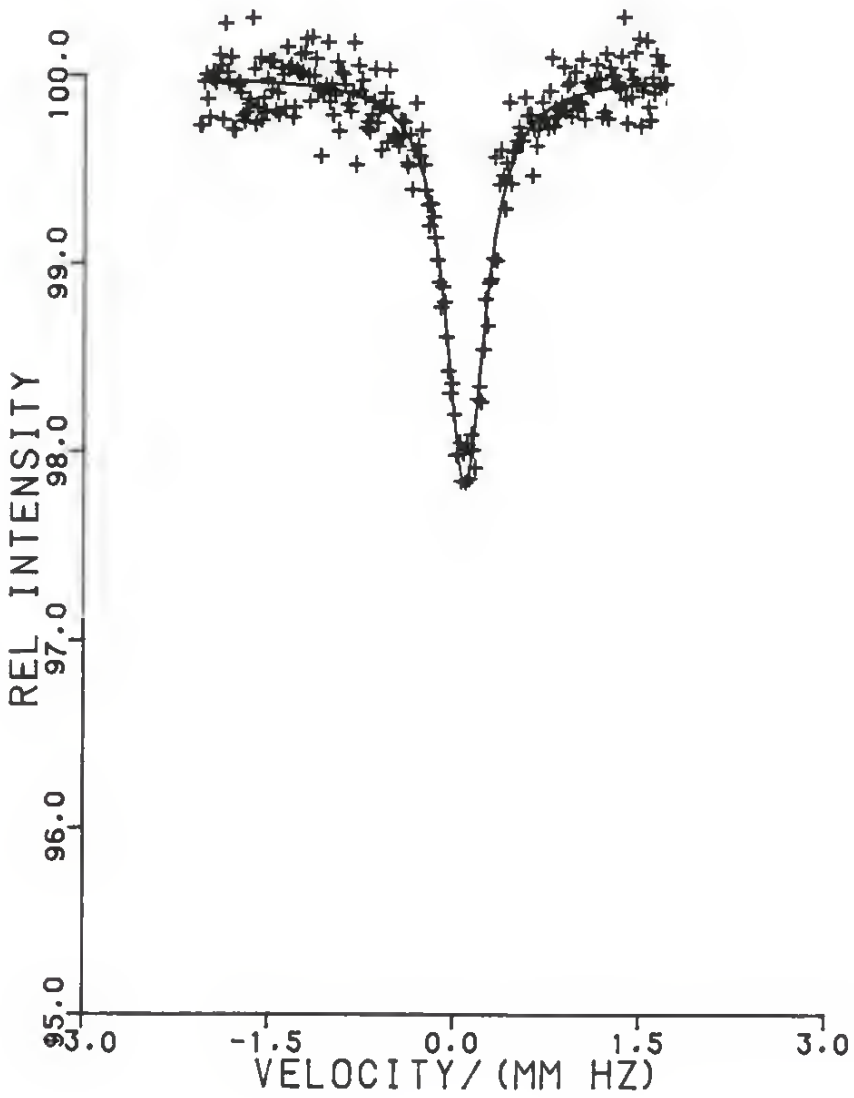

Figure 17. Mossbauer Spectrum of $[Co(phen)_2]_3[Fe(CN)_6]_2$ at 77K

MOSSBAUER SPECTRUM OF
[CO(PHEN)2]3[FE(CN)6]2, 77K
COUNTS =630167.

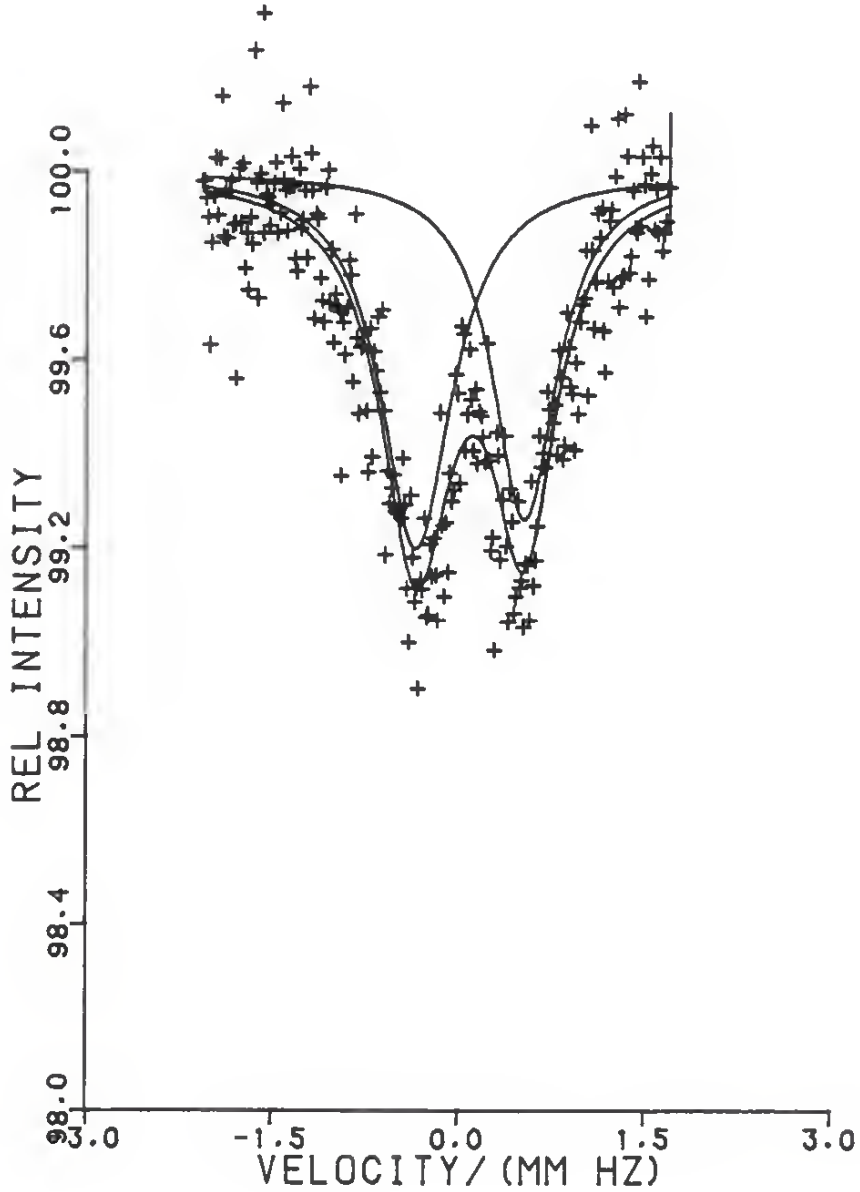

Figure 18. Mossbauer Spectrum of $[Co(phen)_2]_3[Fe(CN)_6]_2$ at 195K

MOSSBAUER SPECTRUM OF
[CO(PHEN)2]3[FE(CN)6]2. 195K
COUNTS =801290.

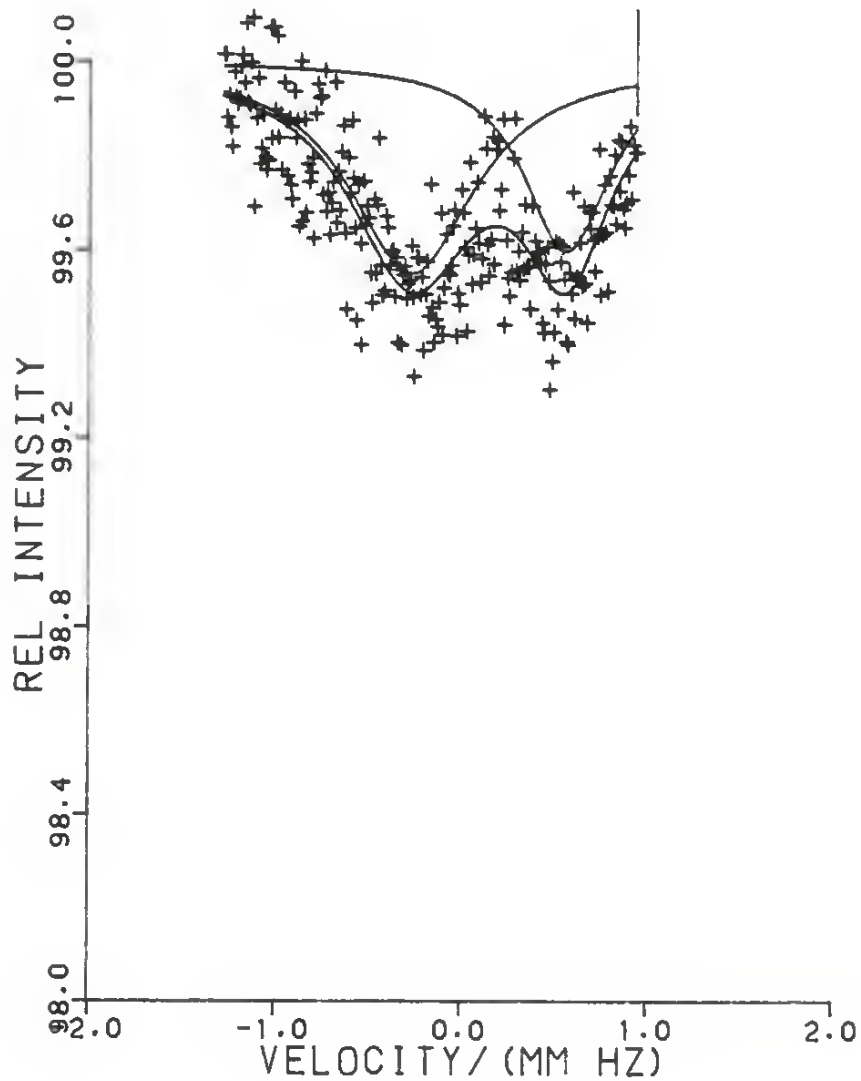

Figure 19. Mossbauer Spectrum of $[Co(phen)_2]_3[Fe(CN)_6]_2$ at 295 K

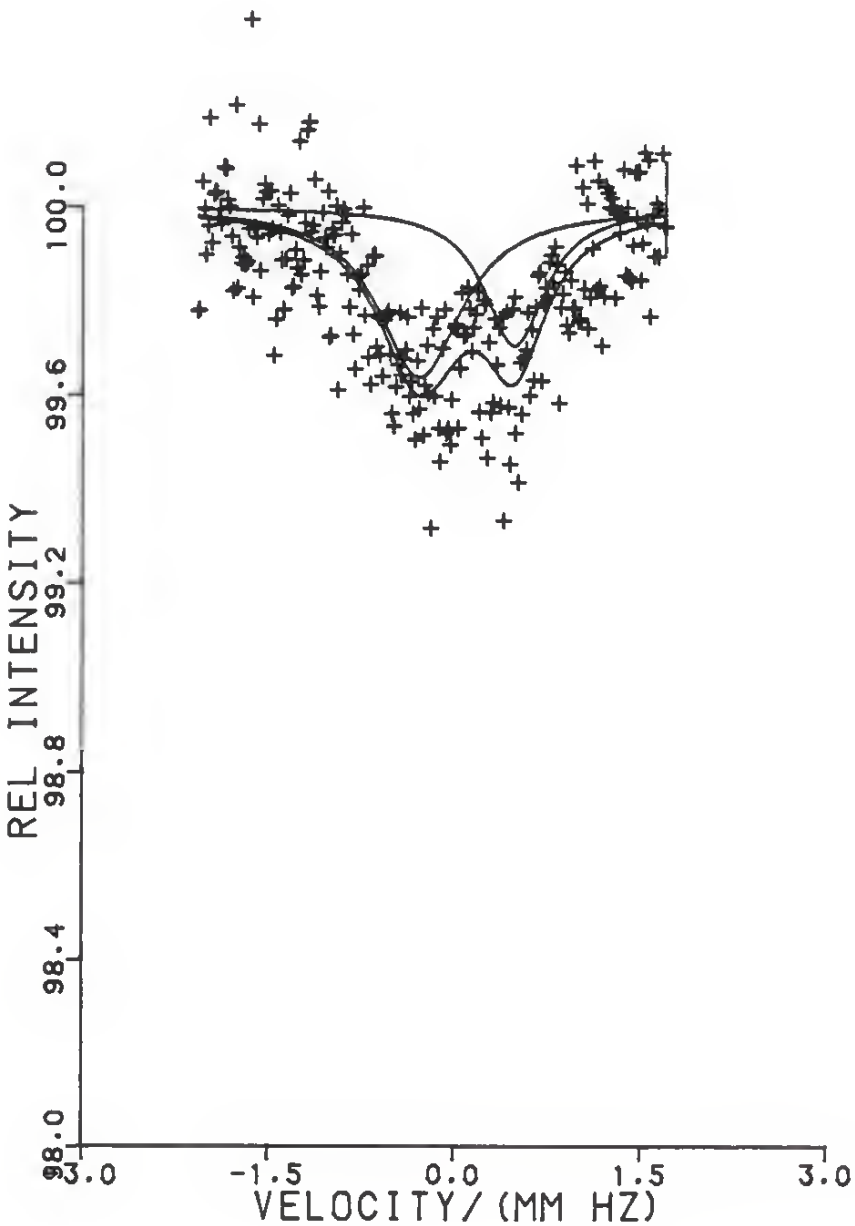
MOSSBAUER SPECTRUM OF
[CO(PHEN)2]3[FE(CN)6]2, 295K
COUNTS =1073972.
REL INTENSITY
100.0
99.6
99.2
98.8
98.4
98.0
-3.0
-1.5
0.0
1.5
3.0
VELOCITY/(MM HZ)

ranging from .8% of the baseline at 77K to .3% at room temperature. The centershift of I*A is at lower energy than that of I, but the difference is not sstatistically significant at room temperature and barely so at 77K. Values for the center shifts for the hydrated form are given in Table 5. The center shifts and the quadrupole splittings for the anhydrous form are in Table 6. Both sets of data are presented graphically in Figures 20-22. No significance should be attached to the variability of the intensities of these spectra, as the sample was not of uniform thickness and it was not positioned in the same way for each spectrum.

Typically, ferricyanide has a small quadrupole splitting. Reported values range from 113 mm/sec to .30 mm/sec[45-48] at room temperature. The more recent, and presumably more reliable, values are in the .25 to .30 mm/sec range. Our own measurement gave a value of .30 mm/sec at room temperature. We find that a sample which is not 'fresh' (having set on the shelf for several years) may give no quadrupole splitting at all, indicating some chemical or physical change of the sample. Apparently the site heterogeniety present smears out the splitting. This is one possible explanation for the lack of splitting in the I*A spectra.

The linewidth of I*A is near 'normal' at room temperature but is nearly twice the normal linewidth at low temperatures. Broad lines are apparent in I at all temperatures.

Table 5. Mossbauer Spectral Parameters for $[Co(phen)_2]_3[Fe(CN)_6]_2*23H_2O$

Temperature (Kelvin)	Center Shift* (mm/sec)	Linewidth (FWHH**) (mm/sec)
77	-.132 (.004)	.567 (.008)
195	-.103 (.005)	.52 (.01)
275	-.091 (.008)	.36 (.01)
295	-.098 (.004)	.387 (.007)

* Referred to Fe matrix source
**Full Width at Half Height, including source line width
The number in parentheses is the standard deviation.

Table 6. Mossbauer Spectral Parameters for $[Co(phen)_3]_3[Fe(CN)_6]_2$

Temperature (Kelvin)	Center Shift* (mm/sec)	Quadrupole Splitting (mm/sec)	Linewidth (FWHH**) (mm/sec)
77	-.08 (.02)	.87 (.02)	.64 (.04)
195	-.04 (.03)	.83 (.03)	.70 (.07)
295	-.06 (.04)	.76 (.04)	.70 (.08)

* Referred to Fe matrix source
** Full width at half height, including source line width
The number in parentheses is the standard deviation.

Figure 20. Effect of Temperature on the Center Shift of $[Co(phen)_2]_3[Fe(CN)_6]_2*23H_2O$

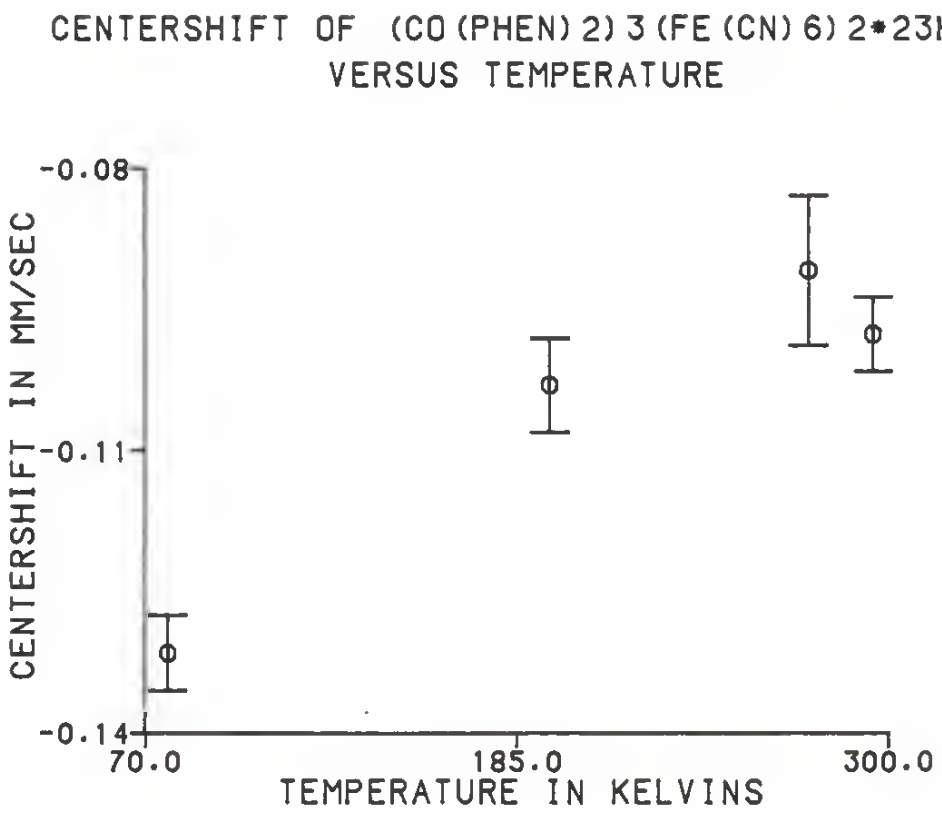
CENTERSHIFT OF (CO(PHEN)2)3(FE(CN)6)2*23H2O
VERSUS TEMPERATURE
-0.08
-0.11
-0.14
CENTERSHIFT IN MM/SEC
70.0
185.0
300.0
TEMPERATURE IN KELVINS

Figure 21. Effect of Temperature on the Center Shift of $[Co(phen)_2]_3[Fe(CN)_6]_2$

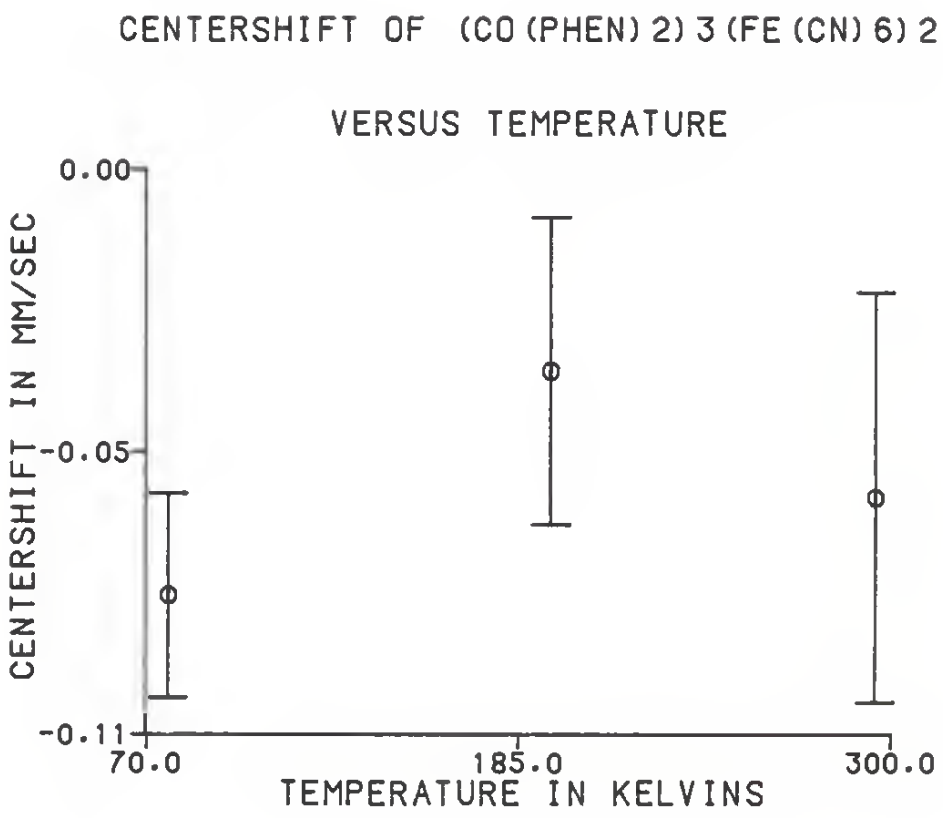
CENTERSHIFT OF (CO(PHEN)2)3(FE(CN)6)2
VERSUS TEMPERATURE
0.00
-0.05
-0.11
CENTERSHIFT IN MM/SEC
70.0
185.0
300.0
TEMPERATURE IN KELVINS

Figure 22. Effect of Temperature on the Quadrupole Splitting of $[Co(phen)_2]_3[Fe(CN)_6]_2$

QUADRUPOLE SPLITTING OF (CO(PHEN)2)3(FE(CN)6)2
VERSUS TEMPERATURE

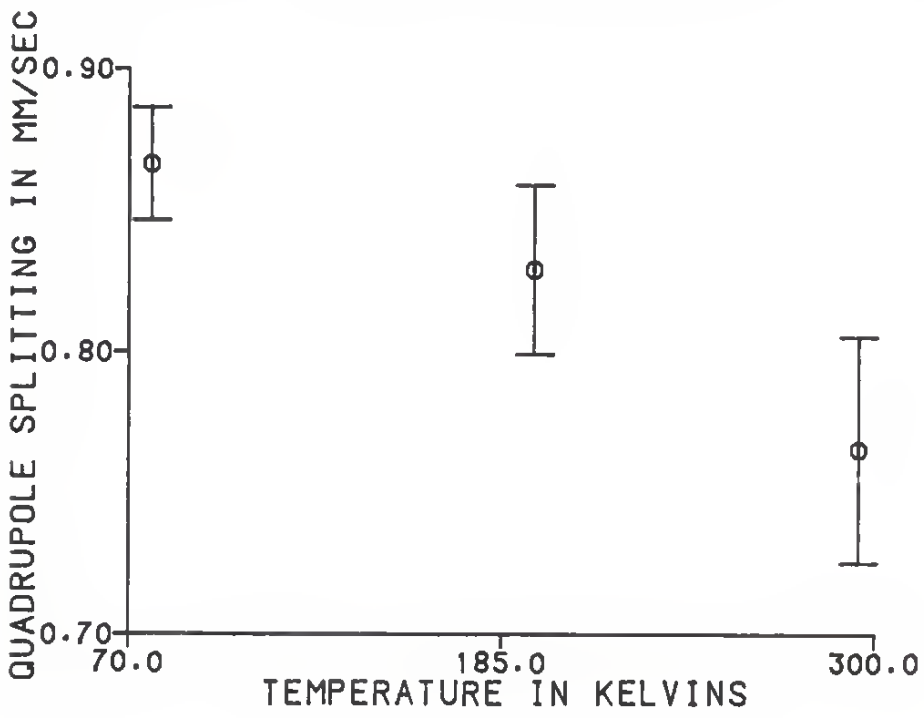

Discussion

The chemical analysis data show that there are five metal centers (two iron and three cobalt atoms) and twelve cyanides per unit of $[Co(phen)_2]_3[Fe(CN)_6]_2*23H_2O$, (I*A); therefore, a +12 charge must be distributed among the five metal centers. Both hexacyano-iron and bisphenanthroline-cobalt comopunds can exist with the central atom in the +2 or the +3 valence state. Table 7 shows the various valence isomers possible among the five metal centers. Of these possibilities, only three result in a total charge of +12;

A) $Co(II)_3Fe(III)_2$,

B) $Co(II)_2Co(III)Fe(II)Fe(Fe(III)$, and

C) $Co(II)Co(III)_2Fe(III)_2$. These are related by a single electron transfer from Co(II) to Fe(III). Our problem is to distinguish among them for both I and I*A.

I*A can be formulated in several ways. The simplest is as a salt with water bonded to the cobalt centers as $[Co(phen)_2(H_2O)_2]_3[Fe(CN)_6]_2*17\ H_2O$ or as some structure in which the cyanides on the iron centers a bridge to the cobalt centers. (These structures are discussed later.) Compound I must have some type of cyano-bridged structure. The striking difference in the magnetic and optical properties of I and I*A suggest that they have markedly different structures; this would lead us to believe that the first structure is correct for I*A. If this is correct, the reversible dehydration of I*Asiust entail a solid-state ligand substitution reaction, as well as a loss of lattice water.

The electron paramagnetic resonance spectra allow isomer C to be eliminated from consideration, for the epr spectra of both I and I*A or

Table 7. Matrix of Possible Total Metal Valence

		Cobalt Valences			
		II,II, II	II,II, III	II,III, III	III,III, III
Iron Valences	II,II	10	11	*12* (Isomer C)	13
	II,III	11	*12* (Isomer B)	13	14
	III,III	*12* (Isomer A)	13	14	15

basically the same as the spectrum for potassium ferricyanide. Since ferrocyanide is diamagnetic and does not have an epr spectrum, we can conclude that isomer C cannot be correct as it contains only Fe(II). No conclusions can be drawn from the epr spectra regarding the cobalt valence isomerism in I and I*A as no resonances attributable to the Co(II) are visible.

The magnetic susceptibility data of I*A can also be used to further reduce the possible electronic structures. Table B shows the possible values of n_{eff} associated with the three possible isomers and the various possible spin states for I and I*A. (n_{eff} is the apparent number of unpaired electrons if the orbital contributions to the magnetic moment are considered. The possible orbital contributions were derived from g parameters for each ion[49]; see Appendix A for details of the calculation. The experimental value for n_{eff} could be affected by ferro- or antiferromagnetic interactions. These were not considered in calculating the ranges in Table 8 as these types of interaction are generally not seen in compounds of this type at or above room temperature). In what follows, we will designate high spin (Co(II) as Co^{2+} and low spin metal ions with a superscript roman numeral, i.e. Co^{II} or Fe^{III}. It should be noted that no values have been tabulated for species which contain Fe^{2+}, Fe^{3+}, or Co^{3+} as it would be extremely unlikely that these species would be found in the high spin form with phen and CN^- ligands coordinated to them. We will first consider I*A, which has the lesser magnetic moment, and then consider I, which has the greater magnetic moment.

I*A has an experimental value for n_{eff} of 5.46 unpaired electrons. Only isomer A has an all low spin configuration for Co(II) which produces a range of n_{eff} which contains the experimental value. n_{eff} for isomer B with

Table 8. Dependence of n_{eff} on the Valence Configuration And Spin State of $[Co(phen)_2]_3[Fe(CN)_6]_2$

	Low Spin	High Spin Number of Cobalts Atoms In High Spin State 1 Co	2 Co	3 Co
Isomer A	5.2-7.1	7.6-10.1	10.0-13.2	12.3-16.2
Isomer B	3.2-4.2	5.5-7.2	7.9-10.2	---
Isomer C	1.1-1.2	3.4-4.3	---	---

one cobalt atom in the high spin configuration also has a range of n_{eff} which contains the experimental value. Furthermore, since only one of the cobalt atoms is high spin, it is still possible for the other two cobalt atoms to undergo transitions to a higher spin state upon dehydration. However, the B electronic configuration contains cobalt atoms in three different electronic states (Co^{II}, Co^{III}, Co^{2+}) in the same molecule, a somewhat bizarre situation. To produce two equivalent cobalt atoms requires either fast Co^{II}/Co^{III} electron transfer or fast Co^{II}/Co^{2+} coupled intersystem crossing. The more troublesome feature of this situation for isomer B would be the presence of one atom each of Co^{II} and Co^{2+}, each with the same coordination sphere.

The high temperature value for n_{eff} indicates 8.06 unpaired electrons. This value is also found for I at room temperature, indicating that the spin state is dependent on the extent of hydration, not on the temperature. Isomer C can be eliminated from consideration (in agreement with the epr data) because the electronic states possible for isomer C require it to contain Co^{3+} or to have values for n_{eff} which do not agree with experimental value. The cases of isomer B with two high spin cobalt atoms and of isomer A with one high spin cobalt atom both have ranges of n_{eff} which contain the experimental value. In both cases, there are two cobalt centers with the same configuration and one with a configuration which is different. (This will have significance when we consider the possible molecular structures.)

In summary: a) isomer C can be eliminated from consideration and b) each of isomer A and isomer B could explain the values of n_{eff} for I and I*A, and they have in common the occurence of Co^{II}. Thus, a first question concerns the feasibility of Co^{II} when coordinated by phenanthroline and/or H_2O or NC^-. Whereas $Co(phen)_3^{+2}$ is known to be high-spin, it is conceivable

that $Co(phen)_2X_2$ may be low spin if the ligands X are weaker α donors and stronger Π donors than phenanthroline. Both NC^- and H_2O meet these criteria. The effect of the rhombic symmetry component imposed on an O_n symmetry scheme by the cis-X ligands could easily lead to Co^{II} by virtue of the energy raising of the metal z^2 orbital due to the tighter phenanthroline bonding in $[Co(phen)_2X_2]^{+2}$ than in $Co(phen)_3^{+2}$, and of the energy lowering of the metal x^2-y^2 orbital due to weakder X_2 bonding (see Figure 23). Note that the X_2 ligands should be quite labile in $[Co(phen)_2X_2]^{+2}$, providing a basis for the hypothesis that I*A contains $[Co(phen)_2(H_2O)]^{+2}$, which readily loses water to form I.

As a second observation at this point, we find Fe^{III} in the presence of Co^{II} and/or Co^{+2}. Sutin and Haim[42] found that K for

$$Fe(CN)_6^{-3} + Co(phen)_3^{+2} \rightleftarrows Fe(CN)_6^{-4} + Co(phen)_3^{+3}$$

is slightly greater than one. Given the rhombic distortion in $[Co(phen)_2X_2]^{+2}$ and the fact that I and I*A are solids, there is no inconsistency here with either the A or the B isomer formulation.

We now turn to the Mossbauer spectral data. Table 9 shows the various possible Mossbauer spectra which would be predicted by the electron configurations under consideration. I*A does not exhibit quadrupole splitting. This is not expected for a molecule containing Fe(III), as do both isomers A and B. Possible explanations are $q = 0$ by fast electric field gradient averaging over rhombically or trigonally distorted Jahn-Teller structures of Fe(III); by heterogeneous environments for Fe(III) (small q required); or by fortuitous cancellation of the valence shell and outer-sphere contributions to q. The width of the resonance line could

Figure 23. Molecular orbital Comparison for $[Co(phen)_3]^{2+}$ and $Co(phen)_2X_2$

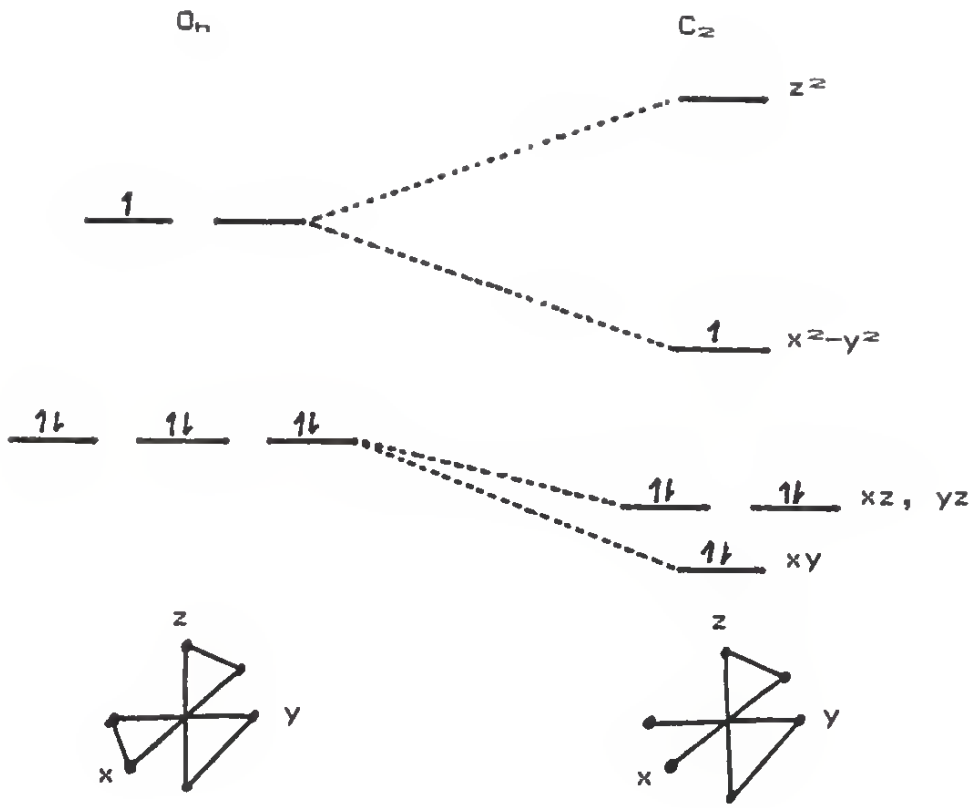
O_h
C_{2v}
z^2
1
1
x^2-y^2
1t
1t
1t
1t
1t
xz, yz
1t
xy
z
y
x
z
y
x

Table 9. ^{57}Fe Bands Predicted From the Field Gradient And Electron Tranfer Possibilities for Isomers A and B

	Equivalent Fe ($q \neq 0 \backslash q = 0$)	Non-equivalent Fe ($q \neq 0 \backslash q = 0$)
Isomer A (Fe_2^{II})	(2\1)	(4\2)
Isomer B ($Fe^{II}Fe^{III}$)	(2\1)*	(3\2)

*fast electron transfer required

support the concept of site heterogeneity, were we able to exclude thickness broadening as the source of the enhanced width.

Be that as it may, there seem to be equivalent iron sites, with q = 0 for I*A. The simplest interpretation is that I*A is isomer A (two equivalent Fe sites) and no bridging cyanides: $[Co(phen)_2(H_2O)_2]_3[Fe(CN)_6]_2 * 17\ H_2O$. Note that all the water is retained in the solid at the temperatures reported here for I*A, and that no significant intersystem crossing has occurred. However, isomer B cannot be definitively eliminated, as fast electron transfer between $[Fe(CN)_6]^{n-}$ sites is possible and could produce collapse of the q tensors by randomization of the Jahn-Teller structures of Fe(III). Isomer B still leaves us with the unusual situation of three different atom configurations (Co^{II}, Co^{III}, Co^{2+}) in the same unit cell.

The Mossbauer spectrum of I is more challenging to interpret. The spectral intensity is reduced from that of I*A by 4x to 10x, although the recoilless fraction need not be reduced that much, since the number of bands has increased from one to two. There is perhaps line broadening from site heterogeneity or a dynamic process. A mixture of both terminal and bridging cyanide ligands accounts for the quadrupole splitting of .8 mm/sec typical values for such structures are .5 to .7 mm/sec). We know that dehydration of the lattice has 'locked in' the higher spin state for the 295K spectrum. Referring to Table 9, and recalling the presence of bridging cyano ligands, which ensure that 1 ≠ 0, the simplest interpretation would be isomer A, with statistically equivalent Fe sites.

To summarize, the Mossbauer data fail to establish cleanly the valences of the iron centers in either I or I*A or Be. The interpretation of the magnetic susceptibility, epr, and Mossbauer data for I and I*A in terms of a

$Co(II)_3Fe(III)_2$ core (isomer A) is straightforward, whereas a core of $Co(II)_2Co(III)Fe(II)Fe(III)$ (isomer B) is consistent with the data only if we postulate fast electron transfer between the Fe sites and fast Co(II)/Co(III) electron transfer or fast Co(II)/Co(II) intersystem crossing.

Turning to the electronic spectra, there are three possible transitions that could account for the IT band in the visible region of I*A: an electron transfer from Co(II) to Co(III), an electron transfer from Fe(II) to Fe(III), or a transfer betwen Co and Fe. The first requires that the compound be formulated as isomer B or C, and the second requires the compound to be isomer B. A transfer between iron and cobalt can occur in any of the three isomers.

It is highly unlikely that the IT bands are due to electron transfer between cobalt atoms. Electron transfer from Co^{2+} results in either Co^{3+} ($\pi^* \rightarrow \pi^*$), which is a doubly excited Co^{III} or a singly excited Co^{III} ($\sigma^* \rightarrow \pi^*$), both of which are highly excited states (the ground state being Co^{III}). A Co^{II} to Co^{III} transition of the ($\sigma^* \rightarrow \sigma^*$) type can be discounted because of poor donor/acceptor overlap. A $\pi^* \rightarrow \sigma^*$ transfer again produces a singly excited Co^{III} of too high energy to accound for the low energy of the IT band.

The transfer of an electron between cobalt and iron may not seem all that plausible at first glance. However, the aqueous half-reactions[28,50]:

$$[Fe(CN)_6]^{-3} + e^- \rightleftarrows [Fe(CN)_6]^{-4} \quad E^o = .36V$$

$$[Co(phen)_3]^{+3} + e^- \quad [Co(phen)_3]^{+2} \quad E^o = .36V$$

indicate that the initial and final state energies may be very similar. This is supported by the work of Sutin and Haim which shows the equilibrium constant to be about 5 for the reaction above with ferrocyanide and $[Co(phen)_3]^{+3}$ as the products[42]. The fact that the E° cited is for $[Co(phen)_3]^{+3}$ instead of $[Co(phen)_2X_2]^{+2}$, and that the E° applied to aqueous solution, and not the solid phase, makes this a rather crude estimate, but it serves to illustrate that an electron transfer from cobalt to iron with an energy corresponding to a visible absorption is a reasonable proposition.

In prussion blue, two IT bands are observed: $Fe^{II}(\pi^*) \rightarrow Fe^{III}(\pi^*)$ (very intense) and $Fe^{II}(\pi^*) \rightarrow Fe^{III}(\sigma^*)$ (very weak)[51]. Their separation (ca. 10,000 cm^{-1} corresponds to a typical $\pi^{*4}\sigma^{*2} \rightarrow \pi^3\sigma^{*3}$ d/d transition in Fe^{2+}. Note that the $\pi^* \rightarrow \pi^*$ transition is very much more intense than the $\pi^* \rightarrow \sigma^*$ band.

In I*A, four IT bands are possible for a Co to Fe transition: $Co(\pi^*) \rightarrow Fe(\sigma^*)$, $Co(\pi^*) \rightarrow Fe(\pi^*)$, $Co(\sigma^*) \rightarrow Fe(\pi^*)$, and $Co(\sigma^*) \rightarrow Fe(\sigma^*)$, of which only the $\pi^* \rightarrow \pi^*$ band should be intense. That is the assignment we make for the IT band at 650 nm. Such a transition is possible for either isomer A ($Co^{II} \rightarrow Fe^{III}$) or isomer B ($Co^{II} \rightarrow Fe^{III}$, $Co^{2+} \rightarrow Fe^{III}$, or $Fe^{II} \rightarrow Fe^{III}$).

The $Co^{II}(\sigma^*) \rightarrow Fe^{III}(\pi^*)$ should lie well below this band by an energy corresponding to a $\pi^{*6} \rightarrow \pi^{*5}\sigma^{*1}$ d/d band in Co^{III}, while a $Co^{2+}(\sigma^*) \rightarrow Fe^{III}(\pi^*)$ band should lie above this band by an energy corresponding to a $\pi^{*4}\sigma^{*2} \rightarrow \pi^{*5}\sigma^{*1}$ d/d band for Co^{3+}. Neither of these transitions, of energies in excess of 10,000 cm^{-1}, can account for the weak band at 520 nm in I*A (the 520 nm band is only 4,000 cm^{-1} above the 420 nm IT band). On the other hand, a $Co^{II}(\sigma^*) \rightarrow Fe^{III}(\sigma^*)$ transition has an energy shift from the IT band given by the difference in $\pi^{*6} \rightarrow \pi^{*5}\sigma^{*1}$ energies for Fe^{II} and Co^{III} and could account for the 520 nm band. (A $Co^{2+}(\sigma^*) \rightarrow Fe^{III}(\sigma^*)$ band has a shift

from the IT band of the sum of the Co^{3+} and Fe^{II} $\pi^{*6} \rightarrow \pi^{*5}\sigma^{*1}$ d/d energies). Another candidate for the 520 nm assignment is the splitting of the $\pi^* \rightarrow \pi^*$ band by the rhombic splitting of the π^* orbitals in $Co(phen)_2X_2$; we reject this possibility on intensity grounds.

As a final conceivable assignment, consider the $Fe^{II}(\pi^*) \rightarrow Fe^{III}(\pi^*)$ transition possible only for isomer B. Expecting a low (0,0) energy for this transition and very little vibrational excitation, it is not reasonable that such a transition could occur at 15,400 cm^{-1} (650 nm).

To summarize, the strong 650 nm band in I*A is assigned to Co^{II} $(\pi^*) \rightarrow Fe^{III}(\pi^*)$ IT transition, and the weak 520 nm band is attributed to a $Co^{II}(\sigma^*) \rightarrow Fe^{III}(\sigma^*)$ transition. We still have no basis for distinguishing between isomers A and B, as these transitions are possible in both formulations.

In the infrared spectrum of ferricyanide salts of simple cations, such as potassium ferricyanide, one sees a single line at 2110 cm^{-1} which corresponds to the t_{1u} CN stretching mode. The t_{1u} band in ferrocyanide salts occurs at much lower wavelength, typically 2060 cm^{-1}. The spectrum of I*A consists of a single intense band at 2045 cm^{-1} and two sidebands at higher energy. The main peak is most likely due to ferricyanide which is not bridging to the cobalt centers. This is consistent with a formulation of I*A as $[Co(phen)_2(OH_2)_2]_3[Fe(CN)_6]_2$*17 H_2O. If the sidebands result from bridging cyano ligands, we may conclude that the lattice is not completely hydrated in the infrared sample. This may be due to the heating effect of the infrared beam.

The curiosity is that the position of the CN band is that typical of ferrocyanide and not ferricyanide, in clear contradiction with the magnetic and epr data, which require the presence of Fe(III). Were it not for these

latter data, one would erroneously conclude from the infrared data alone that I*A is isomer C!

The spectrum of I, as recorded, exhibits three distinct absorption bands. The 2055 band looks suspiciously like the largest peak in I*A. It is most likely to also be due to terminal cyano ligands. This would leave us to assign the two higher energy peaks (2095 and 2120 cm^{-1}) to nonequivalent bridging cyanide ligands. Noting that these peaks are essentially 1:1, one needs to propose structures which the six bridging groups are grouped into two structurally distinct sets of three. Finally, the appearance of the 2100 cm^{-1} bands is consistent, by precedent, with the presence of Fe(III). However, the curiously low energy of the Cn vibrations for the Fe(III) sites of I*A must be recalled.

There are a myriad of possible structures for I. These can be greatly reduced by placing some reasonable restrictions on what structures we will consider. Although bisphenanthroline-cobalt compounds with the phenanthroline ligands in both the cis and trans configurations have been reported, the validity of the existence of the trans form is disputed. It is therefore reasonable to restrict further consideration to the cis conformation. The cis form can exist as both Λ and Δ optical isomers. The reactions involved in the formation of the I*A and I complex should not be stereospecific and both compounds should be racemic mixtures. The ferricyanides have six cyanides available for bonding to cobalt. Stoichiometry tells us that, if every vacant coordination site on the cobalt atoms is filled, on the average each iron will have three bridging cyanides; we will restrict the discussion to those structures which have both iron centers with three bridging cyanides. With these restrictions, there are 68 possible structures of three main types.

Figure 24 shows the most symmetric of the possible structures (D_{3h} point group for the $Co_3[Fe(CN)_6]_2$ frame). Both iron atoms are bonded facially and each cobalt is bonded to a cyanide from each iron. There are four possible isomers, two diastereomers and their enantiomers, resulting from the chirality of the cobalt centers; ΔΔΔ, ΛΛΛ, ΔΔΛ, ΛΛΔ.

The synthesis procedure may or may not achieve resolution of the diasteriomers. One would expect that different solubilities would favor the precipitation of one diasteriomeric pair over the other. The ΔΔΛ, ΛΛΔ pair is favored by entropy as the major product. Whether it would be less soluble than the other diastereomer is not known.

The ΔΔΔ diastereomer would have only two types of CN, bridging and terminal. This is not consistent with the infrared data which requires at least three types of CN. The C_{3h} diasteriomer is also inconsistent with the magnetic data which requires at least two different types of cobalt to account for eight unpaired electrons. The symmetry of the entropy-favored diasteriomer is lowered to C_2 and would permit the presence of two types of cobalt centers. The C_2 form could show a maximum of six different pairs of cyanide groups, three bridging types and three terminal types. Whether the asymmetry of the phenanthroline ligands about the cobalt centers would cause the splitting of the bridging and terminal bands is open to question.

Figure 25 shows chain or linear structures with one central cobalt atom and two terminal cobalt atoms. There are two ways to arrange the terminal cobalt units around each iron center, meridionally and facially with respect to the central cobalt atom. By considering just the stereogeometry around the iron, we can group the isomers of this chain arrangement into three types; with the bridging cyanides arranged facial-facial (ff), 6 isomers; facial-meridional (fm), 8 isomers; and meridional-meridional (mm), 6

Figure 24. "Cage Structure for $[Co(phen)_2]_3[Fe(CN)_6]_2$

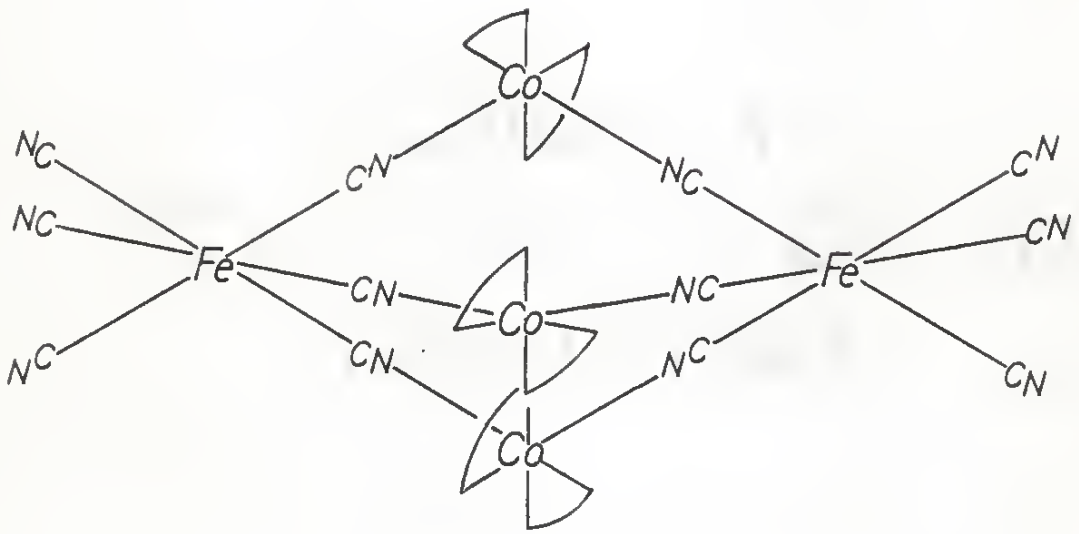
Co
NC
NC
CN
NC
CN
Fe
CN
Co
NC
Fe
CN
CN
NC
CN
NC
Co

Figure 25. "Linear" Structure for

$[Co(phen)_2]_3[Fe(CN)_6]_2$

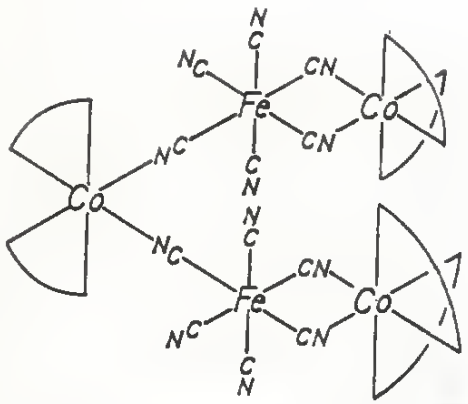

Meridional-Meridional

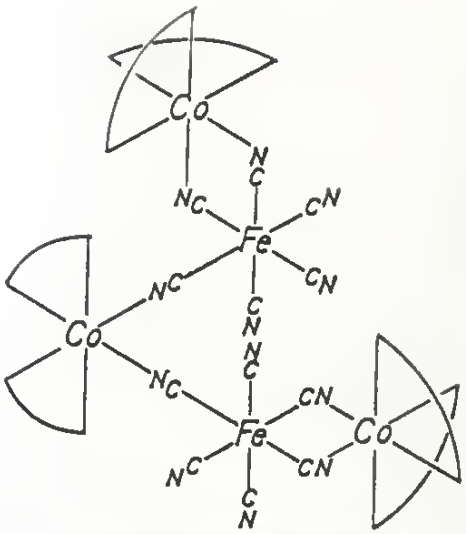

Meridional-Facial

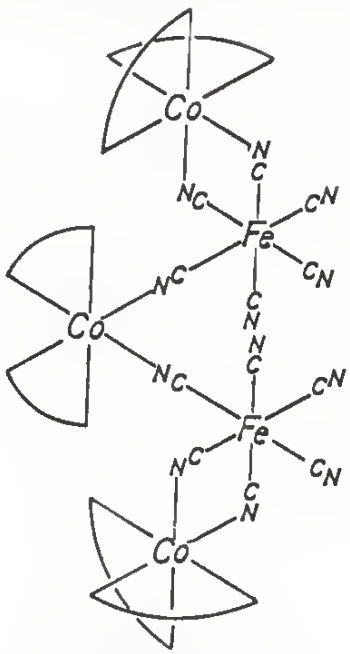

Facial-Facial

Figure 26. Ring Polymer Structure for $[Co(phen)_2]_3[Fe(CN)_6]$

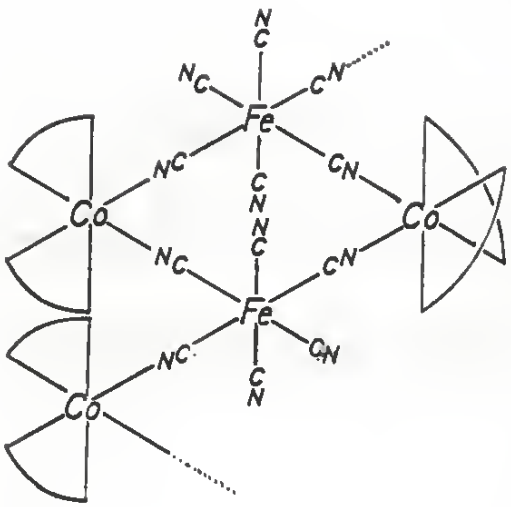
N
C
NC
CN
Fe
NC
CN
C
N
Co
Co
NC
CN
N
C
Fe
NC
CN
C
N
Co

isomers. The mm structure is certainly favored on steric considerations as it allows the terminal cobalt units to stay much farther away from each other than in the other two structures, but all of these structures put strain upon the CN bond because of the angle that is necessary to bond to both iron and the terminal cobalt atoms. (However, this is not unprecedented, as bent CN bridges have been postulated for compounds such as $Fe_2(CN)_{10}$ and $Ni_3(tren)_2(CN)_2$[52,53].) All three stereoisomers of this type have two very different types of cobalt in them which would be consistent with the interpretation of the magnetic susceptibility data. Structures of this type have either six or twelve equivalent types of cyanides, depending on whether a C_2 is present in the molecule or not.

A third possible type of structure is a polymeric one shown in Figure 26. Each monomer unit consists of two cobalt atoms which are bridged by the two ferricyanide units to and from a planar $Co_2Fe_2(CN)_4$ ring. The third cobalt unit is the polymerization linkage between rings. In addition to the meridional-facial isomerism and optical isomerism there is also cis-trans isomerism possible in this type structure, depending on whether the cobalt units which link the rings are on the same side of the central ring or not. Again, ff, fm, and mm structures are possible with the mm structure being somewhat less congested than the other two. The eighteen possible mm structures have six types of cyanides, as a C_2 or S_2 is always present. The sixteen mf structures have no symmetry element and all twelve cyanides are nonequivalent. The ff structures have some symmetry (point groups C_2 or C_1) but are brutally congested as, in order to polymerize, the phenanthroline ligands on the connecting cobalts must be over the ring. The polymer would be terminated by a cage type structure (Figure 24) or a terminal cobalt

unit, such as those in Figure 25. These structures have an advantage over the second type of structure as the cyanides are not required to bend in order to form a bridge. As with the linear structures, there are two very different types of cobalt.

All of the structures considered are listed in Table 10 along with the symmetry elements present and the number of types of cyanides. It is very difficult to eliminate many of these structures definitively, as most would give fairly similar results for the physical measurements which have been made. The cage type ΔΔΔ or ΛΛΛ structures have too much symmetry to account for the infrared data as mentioned before. The linear structures would have to be considered poor candidates because of the bending of the CN's; the cage and ring-polymer structures avoid this problem. The polymer structure may account for the poor crystallization properties of the compound and provides a simple explanation of the two Co sites, in a 2:1 ratio, for I. Still, no definitive answer as to the structure can be made without an X-ray crystal structure determination.

If the scenario for explaining the behavior of the compound is correct, it leads us to the curious result that the IT bands are found in the form of the compound in which the positive and negative ions are unconnected and disappear when bridging ligands connect the species. This is just the opposite of what would be expected, for a bridging ligand usually facilitates electron transfer. This expectation is subject, however, to the requirement that the donor/acceptor orbitals for the IT transition possesses compatible orbital orientation; these orbitals must not be orthogonal. It is possible that the cage structure for I possesses an arrangement of the π^* orbitals involved in the transition which would cause the transition

probability to be very small, however more work must be done to confirm this.

Table 10. Possible Structures for $[Co(phen)_2]_3[Fe(CN)_6]_2$

Type of Structure	Symmetry Elements Present	Types of CN^-
Cage Structures (Figure 24)		
ΔΔΔ	C_3 3 C_2	2
ΔΔΛ	C_2	6
ΔΛΛ	C_2	6
ΛΛΛ	C_3 3 C_2	2
Linear Structures (Figure 25)		
mmΔΔΔ	C_2	6
mmΛΛΛ	C_2	6
mmΔΛΔ	C_2	6
mmΛΔΛ	C_2	6
mmΔΔΛ	none	12
mmΛΛΔ	none	12
mfΔΔΔ	none	12
mfΔΔΛ	none	12
mfΔΛΔ	none	12
mfΔΛΛ	none	12
mfΛΛΔ	none	12
mfΛΔΛ	none	12
mfΔΛΛ	none	12
mfΛΛΛ	none	12
ffΔΔΔ	C_2	6
ffΛΛΛ	C_2	6
ffΔΛΔ	C_2	6
ffΛΔΛ	C_2	6
ffΔΔΛ	none	12
ffΛΛΔ	none	12

Continued.

Table 10 Continued

Type of Structure	Symmetry Elements Present	Types of CN^-
Polymer Structures (Figure 26)		
mm trans△△△	C_2	6
mm trans/\/\/\	C_2	6
mm trans/\/\△	C_2	6
mm trans△△/\	C_2	6
mm trans△/\△△/\/\	i	6
mm trans/\△△△/\/\	i	6
mm cis△△△	C_2	6
mm cis/\/\/\	C_2	6
mm cis△/\△	C_2	6
mm cis/\△/\	C_2	6
mm cis△△/\	C_2	6
mm cis/\/\△	C_2	6
mm cis/\△△	C_2	6
mm cis△/\/\	C_2	6
mf trans△△△	none	12
mf trans△△/\	none	12
mf trans△/\△	none	12
mf trans/\△△	none	12
mf trans△/\/\	none	12
mf trans△/\△	none	12
mf trans/\/\△	none	12
mf trans/\/\/\	none	12
mf cis△△△	none	12
mf cis△△/\	none	12
mf cis△/\△	none	12
mf cis/\△△	none	12
mf cis△/\/\	none	12
mf cis/\△/\	none	12
mf cis/\/\△	none	12
mf cis/\/\/\	none	12

Continued.

Table 10 Continued

Type of Structure	Symmetry Elements Present	Types of CN^-
ff trans△△△	C_2	6
ff trans△△△	C_2	6
ff trans△△△△△△	i	6
ff trans△△△△△△	i	6
ff trans△△△	C_2	6
ff trans△△△	C_2	6
ff cis△△△	C_2	6
ff cis△△△	C_2	6
ff cis△△△	C_2	6
ff cis△△△	C_2	6
ff cis△△△	C_2	6
ff cis△△△	C_2	6
ff cis△△△	C_2	6
ff cis△△△	C_2	6

Summary

1. The compound $[Co(phen)_2]_3[Fe(CN)_6]_2$ exists in both the green hydrated (I*A) and reddish-brown anhydrous (I) forms. The hydrated form is characterized by an IT band in the visible region at 650 nm.

2. A spin crossover occurs when I is hydrated and when I*A is dehydrated. Spin pairing is associated with the formation of green I*A, and spin unpairing with the reddish-brown I.

3. The electronic structure for I*A is either $Co_3^{II}Fe_2^{III}$ or $Co^{II}Co^{2+}Co^{III}Fe^{II}Fe^{III}$. The electronic structure for I is either $Co_2^{II}Co^{2+}Fe_2^{III}$ or $Co_2^{2+}Co^{III}Fe^{II}Fe^{III}$. The simplest interpretation of all the data leads to the former in both cases.

4. The IT band for I*A results from a transition from Co to Fe. The 650 nm band is due to a $\pi^* \rightarrow \pi^*$ transition while the weaker band at 520 nm is probably due to a $\sigma^* \rightarrow \sigma^*$ transition.

5. The structure of I*A is most likely a salt in which water has coordinated to the cobalt atoms. Dehydration leads to a ligand substitution reaction at the cobalt centers to form compound I which contains bridging cyanide ligands. I could have a structure of three main types: a cage, chain or polymer type structure. A most likely structure would be the polymer structure. However, it is possible that the cage structure could account for the absence of the IT band in the anhydrous form.

Literature Cited

1. Powell, H. M., Proceedings of the Chemical Society, 1959, 73.
2. Purcell, K. F., M. P. Edwards, B. Curnutte, and J. S. Eck. Rev. Sci. Instrum., 56(1), 108 (1985).
3. Lynch, F. J., R. E. Holland, and M. Hammermesh, Physical Reviews, 120, 413 (1960); Holland, R. E., F. J. Lynch, G. J. Perlow, and S. S. Hanna, Physical Review Letters, 4, 181 (1960).
4. Werner, A., Z. Anorg. Chem. 12, 46 (1896).
5. Wells, H. L., American Journal of Science, 3, 417 (1922).
6. Stieglitz, J., Proceedings of the National Academy of Science of the United States, 9, 308 (1923).
7. Day, P., Mixed Valence Compounds, D. Reidel Publishing, Boston, p. 3 (1980).
8. Robin, M. B.,and P. Day, Advances in Inorganic and Radiochemistry, 10, 247 (1967).
9. Hush, N. H., Progress in Inorganic Chemistry, 8,, 357 (1967).
10. Robin, M. B., Inorganic Chemistry, 1, 337 (1962).
11. Curtis, J. C., and T. J. Meyer, Journal of the American Chemical Society, 100, 6284 (1978)a.
12. Curtis, J. C., and T. J. Meyer, Inorganic Chemistry, 21, 1562 (1982).
13. Haim, A., and N. Sutin, Inorganic Chemistry, 15, 476 (1976).
14. Asperger, S., I. Murati, and D. Pavlovic, J. Chem. Soc., 1960, 730.
15. Chadwicke, B. M. and A. G. Sharpe, Advances in Inorganic Chemistry and Radiochemistry, 8, 84 (1966).
16. Schwarz, R. and K. Tede, Chemische Berichte, 60, 69 (1927).
17. Jordan, J. and G. J. Ewing, Inorganic Chemistry, 11, 587 (1962).

18. Qureshi, A. M., Journal of Inorganic and Nuclear Chemistry, 31, 2282 (1969).

19. Stevens, J. G. and V. E. Stevens, Mossbauer Effect Data Index, vol. 3, IFI/Plenum, New York, p. 16 (1972).

20. Greenwood, N. N. and T. C Gibb, Mossbauer Spectroscopy, Chapman and Hall, London, p. 170 (1971).

21. ibid.

22. Borshagovskii, B. V., V. I. Goldanskii, G. B. Seifer, and R. A. Stukan, Izv. Akad. Nauk SSSR Ser Khim, 1968, 87.

23. Borshagovskii, B. V., V. I. Goldanskii, G. B. Seifer, and R. A. Stukan, Izv. Akad. Nauk SSSR Ser Khim, 1968, 1716.

24. Greenwood, N. N. and T. C. Gibb, Mossbauer Spectroscopy, Chapman and Hall, London, p. 170 (1971).

25. Matas, J. and T. Zemcik, Physical Letters, 19, 111 (1965).

26. Adams, D. M., Metal Ligand and Related Vibrations, Edward Arnold LTD, London, p. 170 (1967).

27. Borshagovskii, B. V., V. I. Goldanskii, G. B. Seifer, and R. A. Stukan, Izv. Akad. Nauk SSSR Ser Khimm, 1968, 87.

28. Alexander, J. J. and H. B. Gray, Journal of the American Chemical Society, 90, 4262 (1968).

29. Gray, H. B., and N. A. Beach, Journal of the American Chemical Society, 90, 2922 (1963).

30. Kolthoff, I. M. and W. J. Tomsicek, Journal of Physical Chemistry, 39, 945 (1935).

31. Hanania, G. T., D. H. Irvine, W. A. Eaton, and P. George, Journal of Physical Chemistry, 71, 2022 (1967).

32. Blau, F., Monatsheft fur Chemie, 19, 647 (1898).

33. Irving, H. and D. P. Mellor, Journal of the Chemical Society, , 5222 (xxxx).

34. Taube, H., Chem. Rev., 50, 69 (1952).

35. Ellis, P. G., and R. G. Wilkins, Journal of the Chemical Society, 1959, 299.

36. Ellis, P. G., R. G. Wilkins, and M. J. G. Williams, Journal of the Chemical Society, 1957, 4456.

37. Schilt, A. A., and R. C. Taylor, Journal of Inorganic and Nuclear Chemistry, 9, 220 (1959).

38. Kiss, A. and J. Csaszar, Acta Chim. Acad. Sci. Hung., 38, 405 + 421 (1963).

39. Gil, L., E. Moraga, and S. Bunel, Molecular Physics, 12, 333 (1967).

40. Lee, C. S., H. M. Neumann, and H. R. Hunt, Inorganic Chemistry, 5, 1397 (1966).

41. Paglia, E. and C Sironi, Gazzetta chimica italiana, 88, 541 (1958).

42. Salvadeo, P., Gazzetta chimica italiana, 89, 2184 (1959).

43. Galbraith Laboratories, Inc., P. O. Box 4187, 232 Sycamore Drive, Knoxville, Tn. 37921.

44. Angelici, R. J., Synthesis and Technique in Inorganic Chemistry, W. B. Saunders Company, Philadelphia, p. 42, (1969).

45. Garg, A. N. and P. S. Goel, Journal of Inorganic and Nuclear Chemistry, 31, 697 (1969).

46. Costa, N. L., J. Danon, and R. M. Xavier, Journal of Physics of Chemical Solids, 23, 1783 (1962).

47. Brady, P. R., J. F. Duncan, and K. F. Mok, Proceedings of the Royal Society (London), A287, 343 (1965).

48. Valor, P. M., V. K. Sokolova, A. S. Vilenskii, and E. E. Vainshtein, Pribory I. Tekhn. Eksperim., 10, 161, (1965).

49. Purcell, K. F. and J. C. Kotz, Inorganic Chemistry, p. 578, W. B. Saunders Company, Philadelphia, (1977).

50. Paglia, E. and C. Sironi, Gazzetta chimica italiana, 87, 1125 (1957).

51. Robin, M. B., Inorganic Chemistry, 1, 337 (1962).

52. Emschwiller, G., and C. K. Jorgenson, Chemical Physics Letters, 5, 561 (1970).

53. Mann, K.R., D. M. Duggan, and D. N. Hendrickson, Inorganic Chemistry, 14, 2577 (1975).

Appendix A

The magnetic moment which is due only to the spin of the electrons is related to the spin angular momentum of the electrons as:

$$1 \quad U_{so} = g_s B_e [S(S+1)]^{1/2}$$

where g_s is the magnetogyric ratio and is approximately equal to 2.0, B_e is the Bohr magneton which is equal to $9.27 * 10^{-21}$ erg/gauss and S is the total spin angular momentum quantum number of the system. Systems often have a contribution to the magnetic moment due to the orbital angular momentum in addition to the spin-only component. In order to facilitate the handling of these situations, g is allowed to become a parameter defined as:

$$2) \quad G_{obs} = U_{obs}/B_e[S(S+1)]^{1/2} = U_{eff}/[S(S+1)]^{1/2}$$

$$= G_s U_{obs}/U_{uSO}$$

where U_{obs} is the observed magnetic moment.

By substituting minimum and maximum values observed values for g (see Purcell and Kotz[49]), it is possible to calculate from equation 2, the minimum and maximum values for U_{eff} for a given electron configuration of a metal center. Since S = n/2, where n is the number of unpaired electrons, we can show that n_{eff} is related to u_{eff} as:

$$3) \quad N_{eff}2 + 2n_{eff} = (2u_{eff}/g_s)^2$$

Using the quadratic formula, this equation can now be solved for the range of n_{eff} values corresponding to the range of u_{eff} values. Replacing g_{obs} by g_s in equation 2 allows one to obtain the n_{eff} value for the new compound, for a comparison of nominal ranges.

A STUDY OF THE MAGNETIC PROPERTIES OF AND INTERVALENCE ELECTRON TRANSFER IN $[Co(phen)_2]_3[Fe(CN)_6]_2*23H_2O$

by

R. David Jones
B. A., Monmouth College, 1982

AN ABSTRACT OF A MASTER'S THESIS

submitted in partial fulfillment of the
requirements for the degree

MASTER OF SCIENCE

Department of Chemistry

KANSAS STATE UNIVERSITY

Manhattan, Kansas

1985

Abstract

$[Co(phen)_2]_3[Fe(CN)1]_2*23H_2O$ (I*A) and the anhydrous form of the same compound (I) were synthesized and studied. I*A is a green microcrystalline solid which dehydrates easily microcrystalline solid which dehydrates easily (60°C) to form I which is reddish-brown, the color change is quite striking.

Variable temperature magnetic susceptibility measurements and epr, visible, infrared, and Mossbauer spectra were obtained for both forms. The magnetic susceptibility measurements showed that a spin crossover occurs which is dependent on the extent of hydration. I*A shows an effective magnetic moment of 6.38 Bohr magnetons while I shows an effective magnetic moment of 9.0 Bohr magnetons. The epr data confirm the presence of Fe(III) centers in the complex.

I*A shows a Mossbauer spectrum with a single brad line while I shows a broad doublet with a quadrupole splitting of .87 mm/sec at 77K. From these measurements one can deduce that the electronic structure of the metal centers for both I and I*A is either $Co(II)_3Fe(III)_2$ or $Co(II)_2Co(III)Fe(II)Fe(II)$.

The color in I*A is due to intervalence transitions at 650 nm and 520 nm. The band at 650 nm is most likely due to a $Co(II)\pi^* \rightarrow Fe(III)\pi^*$ transition and the weaker band at 520 nm is assigned to a $Co(II)\alpha^* \rightarrow Fe(III)\alpha^*$ transition. These transitions are not seen in I.

The probable structure of I*A is $[Co(phen)_2(H_2O)_2]_3[Fe(CN)1]_2*17H_2O$. Dehydration causes a solid state ligand substitution reaction in which the cyanide ligands bridge to the cobalt centers. This leads to the curious result that the IT bands disappear when there are bridging ligands between the transition centers. Possible structures are of three main types, cage structures, linear structures, and ring-polymer structures. It is possible that the cage structure has an orbital alignment for which the transition is forbidden.